

We would like to thank the reviewers for the valuable comments and suggestions that improved the manuscript. A point-by-point reply to the comments of both reviewers is provided below with the original comments shown in blue.

Reviewer #1 (anonymous)

The paper describes the addition of the bulk conductivity (BC) model into the JULES Land-surface model. The authors have implemented this very simple model in attempts to improve the simulation of chalk hydrology. The BC model is calibrated and shown to improve the simulated mass and energy fluxes over the Kennet catchment. The authors conclude by commenting on the potential suitability of this simple model for large scale land-surface modelling.

It is clear that the authors have taken the time to properly implement the comments and suggestions from the first pass of reviews which have greatly improved the manuscript. The rewording of the title and abstract highlight the strength of the simplicity of the approach, and the calibration of the BC model parameters makes for a much cleaner and more convincing study.

- We would like to thank the reviewer for the encouraging comments.

I have found the paper clunky to read in places. Some restructuring could help improve the readability of the manuscript.

- We have re-structured the manuscript as suggested by the reviewer in the “Minor Comments” section below to improve readability.

Personally I feel that the calibration step needs to be clearer. The calibration step is not mentioned in the Abstract or Introduction of the paper. The word evaluation is used in places where ‘calibration’ would be more relevant. The BC model is first calibrated using soil moisture data at a point scale. The calibrated model performance is assessed and compared to the performance of the default JULES parameterization. Finally it is evaluated against independent data at a catchment scale.

- We thank the reviewer for this valuable comment. We have incorporated the calibration step in the introduction of the revised manuscript (L. 75-82 in manuscript_revised.pdf):

“At the point-scale, the proposed parameterization is calibrated using observed soil moisture profile data. This is achieved by randomly sampling the parameter space and extensively running the model in order to minimize the differences between observed and simulated soil moisture variability at different depths. Finally, the proposed model is applied to the Kennet catchment in the Southern England and the fluxes and states of the hydrological cycle are simulated for multiple years. The simulation results are evaluated using observed latent heat flux (LE) and runoff data to assess the performance of the BC model in simulating land surface processes at the catchment scale.”

Minor Comments

Introduction: It is worth mentioning in the introduction what default JULES does, this becomes clearer later but a sentence here to the effect: ‘JULES has nothing in place for chalk’ would be useful.

- We have incorporated this comment in the introduction of the revised manuscript (L. 71-74 in manuscript_revised.pdf):

“In order to test the proposed parameterization, the BC model is included in JULES (version 4.2), which, by default (i.e., uniform soil column representation using general soil database as typically applied in land surface models), does not represent any chalk feature.”

Pg 4 line 65: ‘...relatively large number of parameters’ could be worth stating how many to contrast with the three parameter model described in the paper.

- We have mentioned the number of parameters used in relevant previous studies in the revised manuscript (L. 48-52 in manuscript_revised.pdf):

“The physics-based models mentioned above were developed based on dual-continua approach and required relatively large numbers of parameters (i.e., on the order of 20-30 parameters) that were calibrated via inverse modelling using observed soil moisture and matric potential data [e.g., *Ireson et al.*, 2009; *Mathias et al.*, 2006].”

Pg 3 line 69: ‘At the point-scale the BC model is evaluated using observed soil moisture data.’ maybe use calibrated instead of evaluated.

- Updated in the revised manuscript (L. 76 in manuscript_revised.pdf):

“At the point-scale, the proposed parameterization is calibrated using observed soil moisture profile data.”

Pg 4 line 87: the units for K_s are inconsistent with the units found in table 3.

- We have used m m d^{-1} as the unit of K_s consistently in the revised manuscript (e.g., L. 97, L. 248-250, Table 2 and Table 3 in manuscript_revised.pdf)

Pg 5 line 105: it is not clear how Price et al.’s values of 3-5 m m d^{-1} for K_s imply a range of 0.8-86 m m d^{-1} for calibration.

- We thank the reviewer for pointing out this important issue. Note that we have chosen a different range of K_s in the revised manuscript following the suggestions of the other reviewer (Dr. Andrew Ireson). While *Ireson et al.* [2009] suggested a range of 0.2-2.0 m m d^{-1} , *Price et al.* [1993] argued that K_s is around 3-5 m m d^{-1} for most chalk soils. Therefore, we consider a range of 0.2-5.0 m m d^{-1} in the revised manuscript for K_s calibration. This updated range of K_s has been discussed in the revised manuscript (L. 248-250 in manuscript_revised.pdf):

“*Ireson et al.* [2009] suggested a range of 0.2-2.0 m m d^{-1} for K_s . On the other hand, *Price et al.* [1993] argued that in general, K_s is around 3-5 m m d^{-1} for most chalk soils. Therefore, we consider a range of 0.2-5.0 m m d^{-1} in optimizing K_s .”

Pg 5 lines 112-123: Please consider moving the calibration description into the methodology.

- We have moved the description of calibration strategy to the “Methods” section (section 3.5) in the revised manuscript (L. 236-260 in manuscript_revised.pdf).

Pg 8 line 189 or Pg 10 line 223: Consider discussing the choice of using the default JULES parameters in the configuration. It is not too surprising that the calibrated parameterization of BC model would outperform an uncalibrated JULES model. The authors address this point in the first pass of reviews but I feel some of the text would benefit from being in the

text. Especially since it highlights the BC model's application to a completely 'naive' model setup.

- We have explained the choice of the parameters in the *default* configuration and the fact that it represents a naïve model configuration deprived of model calibration and chalk representation in the revised manuscript (L. 217-220 in manuscript_revised.pdf):

"In this configuration, each soil column in JULES is considered to be vertically homogeneous with the soil properties defined in Table 2, which is motivated by the Met Office JULES Global Land 4.0 configuration described in *Walters et al. [2014]*."

(L. 231-234 in manuscript_revised.pdf):

"It should also be emphasized that *default* represents a "naïve" configuration deprived of model calibration. Moreover, this configuration does not represent chalk, which, according to previous studies [e.g., *Le Vine et al., 2016*], substantially affects the hydrology of the study area considered here."

Fig 1b): The 'Bare soil', 'Needleleaf' and 'Broadleaf' colours are very similar and hard to distinguish.

- Figure 1b is updated in the revised manuscript to make the colours distinguishable.

Fig 4 (panels (b) to (c)): It would help to shade the bars of the unchanged values differently so that the changes in parameter values becomes more obvious. These panels also don't get discussed much in the main text.

- We have shaded the bars representing uncalibrated and calibrated parameter values using blue and red colours, respectively in Figure 4 of the revised manuscript. We have also enhanced the discussion on Figure 4b, c and d in the revised manuscript (L. 300-313 in manuscript_revised.pdf).

Pg 12 line 271-276: The sensitivity of S_o is particularly interesting and in turn the model doesn't seem sensitive to f_m . I feel the sensitivity of the parameters could be further discussed. Why is it advantageous to use the macro configuration with the two optimized parameters vs the three optimized parameters?

- We have enhanced the discussion on the sensitivity of parameters on model performance in the revised manuscript (L. 282-299 in manuscript_revised.pdf). We have also discussed the benefit of reduced model complexity (i.e., reduced number of parameters for calibration) and our choice of parameters for calibration (i.e., K_s and S_o) in the revised manuscript (L. 293-299 in manuscript_revised.pdf):

"Arguably, the BC model can be implemented in other chalk regions by constraining only S_o parameter. Such result could potentially be advantageous for transferability to other regions in the UK in order to assess chalk hydrology at large-scale. However since this is the first time the BC model is introduced, we decide to take a conservative approach and select the *macro* configuration with optimized K_s and S_o ($macro_{opt}$ hereafter) to simulate chalk hydrology over the study area that ensures best overall model performance."

(L. 408-415 in manuscript_revised.pdf):

"Our results indicated that S_o is by far the most influential parameter in the model when representing water movement through a soil-chalk column. This highlights the simplicity of

the proposed BC model for large-scale studies and potential ease in transferability. In comparison, K_s and f_m showed secondary (low) sensitivity on the model performance. Since this study introduces the BC model, we decided however to take a conservative approach. We optimized K_s and S_o simultaneously for our catchment scale simulations since this combination resulted in the best overall model performance.”

Table 3: there seems to be a lack of consistency between Figure 4 and Table 3. In the text (line 276) ‘... we select the macro configuration with optimized K_s and S_o ...’ which should mean f_m remains unchanged. However in Table 3, f_m ’s optimized value differs for its unoptimized value. The value for f_m in this table might be from optimising over this parameter alone, but then the other parameters have optimized values which differ from their single optimisation value (e.g. K_s). What optimized values are shown in this table? Surely the values used in macro opt should be represented here.

- We thank the reviewer for raising this important issue. We agree that the values presented in Table 3 of the previous manuscript were not consistent with our choice of parameters for calibration (i.e., K_s and S_o). We have updated Table 3 in the revised manuscript (P. 27 in manuscript_revised.pdf). Note that in updated Table 3, calibrated value for K_s (0.31 mmd^{-1}) and S_o (0.46) are presented, while f_m (10^5) remains uncalibrated.

A further comment on Fig.4 and Table 3: what are the units of K_s ? In figure they are of order $\times 10^{-4}$, in the table units (m d^{-1}) and earlier in the text (mmd^{-1}).

- We have updated Figure 4 and added units of K_s (mmd^{-1}) in the revised manuscript (P. 31 of manuscript_revised.pdf). The unit of K_s in Table 3 of the revised manuscript is also updated to mmd^{-1} (P. 27 in manuscript_revised.pdf).

Table 3: Add ranges over which the parameters were allowed to vary in calibration stage.

- Ranges are added in Table 3 of the revised manuscript (P. 27 in manuscript_revised.pdf).

Pg 13 line 196: It is worth commenting that it is still an underestimate.

- Note that this sentence along with the associated figure (i.e., Figure 6 in the previous manuscript) is removed from the revised manuscript. In manuscript_revised.pdf, we focus on the simplicity of the BC parameterization and the calibration of the model parameters to reduce the differences between observed and simulated soil moisture variability based on the comments by Dr. Andrew Ireson during the previous rounds of review. The results show that the calibrated model improves simulated key hydrological processes over the Kennet catchment compared to the *default* configuration. Therefore Figure 6 (previous manuscript) is no longer necessary because all the relevant information (i.e., the comparison between observed and simulated soil moisture variability) is shown in Figure 5 of manuscript_revised.pdf.

Pg 16 line 375: Two parameters vs the three referenced in the rest of the paper... is K_s no longer considered a parameter in the conclusion?

- We would like to thank the reviewer for pointing out this issue. This discussion on the model parameters is clarified in the revised manuscript (L. 403-415 in manuscript_revised.pdf):

“The proposed BC model is a single continuum approach of modelling preferential flow [e.g., *Beven and Germann, 2013*] that involves only 3 parameters, namely the saturated hydraulic conductivity of chalk matrix (K_s), macroporosity factor (f_m) and relative saturation threshold (S_o). Initially, these parameters were estimated from existing literature to assess the

performance of the uncalibrated BC model. Finally, the BC model parameters were optimized to minimize the differences between observed and simulated soil moisture variability. Our results indicated that S_o is by far the most influential parameter in the model when representing water movement through a soil-chalk column. This highlights the simplicity of the proposed BC model for large-scale studies and potential ease in transferability. In comparison, K_s and f_m showed secondary (low) sensitivity on the model performance. Since this study introduces the BC model, we decided however to take a conservative approach. We optimized K_s and S_o simultaneously for our catchment scale simulations since this combination resulted in the best overall model performance.”

Fig 6: Consider adding vertical lines between the bins to highlight the fact the boxplots are of the same depth. This is not immediately clear and I've noticed that reviewer 3 also mentioned the slight confusion caused by this figure.

- As mentioned above, this figure is removed from the revised manuscript.

Reviewer #2 (Dr. Andrew Ireson)

The paper is much improved, and I think that this is a useful contribution. However, there is a lingering problem that really should be addressed before the paper can be published. The authors have misinterpreted the hydraulic conductivity in the LeVine Paper (cited in the manuscript), which was a bulk hydraulic conductivity and not a matrix conductivity. Moreover, in the optimisation of K, the authors have not sampled K on a log-scale (unless they have and have neglected to say this), meaning that the optimized K is biased towards higher values. As a result, I believe the authors still have a matrix K which is unrealistically large compared with other published estimates. In my opinion, this is important and should be corrected before this paper can be published, which unfortunately means re-running the models.

- We would like to thank the reviewer for his valuable suggestions. In the revised manuscript, we have selected a different range for K_s calibration based on relevant previous studies. While *Ireson et al.* [2009] suggested a range of 0.2-2.0 m m^{-1} , *Price et al.* [1993] argued that K_s is around 3-5 m m^{-1} for most chalk soils. Therefore, we consider a range of 0.2-5.0 m m^{-1} in the revised manuscript for K_s calibration. This updated range of K_s has been discussed in the revised manuscript (L. 248-250 in manuscript_revised.pdf):

“*Ireson et al.* [2009] suggested a range of 0.2-2.0 m m^{-1} for K_s . On the other hand, *Price et al.* [1993] argued that in general, K_s is around 3-5 m m^{-1} for most chalk soils. Therefore, we consider a range of 0.2-5.0 m m^{-1} in optimizing K_s .”

Another significant error, though easily fixed, is that the revised manuscript still does not include a plot of runoff for the catchment scale application. Such a plot was included in the response to reviewers (Figure R2 in the response), so should be incorporated into the manuscript. I think that the performance in this figure was reasonable. They should also show the default model performance.

- We thank the reviewer for highlighting this positive result from our study. As suggested, we have incorporated the comparison between observed and simulated runoff (for both *default* and *macro_{opt}*) in the revised manuscript (Figure 8b, L. 360-368 in manuscript_revised.pdf).

If this can be quickly addressed, this will be a nice paper.

I have also identified some minor errors to be corrected, below:

L 65 - "numbers of parameters"

- Corrected in the revised manuscript (L. 50 in manuscript_revised.pdf):

L 80 - to be rigorous you should also show what "K_sb" is when S <= S_o.

- Updated in the revised manuscript (L. 90 in manuscript_revised.pdf)

L 87 - I believe the authors have misinterpreted the LeVine paper, which has a bulk saturated hydraulic conductivity of 16 mm/d, and not a matrix hydraulic conductivity. This number is at least an order of magnitude too high (see e.g. Ireson et al 2009, Price et al 1993, Price et al 2000, Brouyere 2006, all cited in the manuscript).

- As discussed earlier, we have selected a different range for K_s calibration (0.2-5.0 m m^{-1}) based on relevant previous studies as suggested by the reviewer (L. 248-250 in manuscript_revised.pdf):

“Ireson et al. [2009] suggested a range of 0.2-2.0 m m^{-1} for K_s . On the other hand, Price et al. [1993] argued that in general, K_s is around 3-5 m m^{-1} for most chalk soils. Therefore, we consider a range of 0.2-5.0 m m^{-1} in optimizing K_s .”.

Table 2 & 3 should probably use the same units for hydraulic conductivity - m/d is good.

- Updated in the revised manuscript (P. 27 in manuscript_revised.pdf).

Figure 1 c) has 5 colours, while only 3 legend items.

- Updated in the revised manuscript (Figure 1 in manuscript_revised.pdf).

Figure 4 - Need to label the units of K - and what are these? Not mm/d or m/s as far as I can tell - maybe mm/s? Better to use m/d.

- Unit (m m^{-1}) is added in the revised manuscript (Figure 4 in manuscript_revised.pdf).

L 106 - the range in K_s considered is good, though I would expect the true value to be right at the bottom of this range. Did you sample K_s in log-space? I assume not - which is a problem as it will bias your sampling to the higher values. This is important - you need to sample in log-space. I think your default and optimized K_s are still too high (i.e. values in Figure 4). Other than this, the optimization approach is good.

- We have sampled K_s in log space in the revised manuscript (L. 256-257 in manuscript_revised.pdf):

“Note that for the K_s parameter, the random sampling was performed from a logarithmic distribution [Ireson et al., 2009].”

1 **Towards a simple representation of chalk hydrology in land**
2 **surface modelling**

3 **Mostaquimur Rahman¹, Rafael Rosolem^{1,2}**

4 ¹Department of Civil Engineering, University of Bristol, Bristol, UK

5 ²Cabot Institute, University of Bristol, Bristol, UK

6 **Abstract**

7 Modelling and monitoring of hydrological processes in the unsaturated zone of chalk, a
8 porous medium with fractures, is important to optimize water resources assessment and
9 management practices in the United Kingdom (UK). However, incorporating the processes
10 governing water movement through chalk unsaturated zone in a numerical model is
11 complicated mainly due to the fractured nature of chalk that creates high-velocity preferential
12 flow paths in the subsurface. In general, flow through chalk unsaturated zone is simulated
13 using dual-porosity concept, which often involves calibration of relatively large number of
14 model parameters, potentially undermining applications to large regions. Therefore, this
approach may be not be suitable for large scale land surface modelling applications. In this
15 study, a simplified parameterization, namely the Bulk Conductivity (BC) model is proposed
16 for simulating hydrology in chalk unsaturated zone. This new parameterization introduces
only two additional parameters (namely the macroporosity factor and the soil wetness
threshold parameter for fracture flow activation) and uses the saturated hydraulic
conductivity from chalk matrix. The BC model is implemented in the Joint UK Land
21 Environment Simulator (JULES) and applied to a study area encompassing the Kennet
22 catchment in the Southern UK. This parameterization is further calibrated at a point-scale
23 using soil moisture profile observations. The performance of calibrated BC model in JULES
24 is assessed and compared against the performance of both the default JULES

25 parameterization and the uncalibrated version of BC model implemented in JULES. Finally,
26 the model performance at the catchment-scale is evaluated against independent data sets. The
27 simulation results are evaluated using field measurements and satellite remote sensing
28 observations of various fluxes and states of the hydrological cycle (e.g., soil moisture, runoff
29 and latent heat flux) at two distinct spatial scales (i.e., point and catchment). The results
30 demonstrate that the inclusion of the BC model in JULES improves simulated land surface
31 mass and energy fluxes over the chalk-dominated Kennet catchment. Therefore, the simple
32 approach described in this study may be used to incorporate the flow processes through chalk
33 unsaturated zone in large-scale land surface modelling applications.

34 **Keywords:** Chalk hydrology, macroporosity, land surface model, bulk conductivity model.

35 1. Introduction

36 Chalk can be described as a fine-grained porous medium traversed by fractures [Price *et al.*,
37 1993]. Previous studies showed that the unsaturated zone of the chalk aquifers plays an
38 important role on groundwater recharge in the UK [e.g., Lee *et al.*, 2006; Ireson *et al.*, 2009].
39 Therefore, both monitoring [e.g., Bloomfield, 1997; Ireson *et al.*, 2006] and modelling [e.g.,
40 Bakopoulou, 2015; Brouyère, 2006; Ireson and Butler, 2011, 2013; Sorensen *et al.*, 2014]
41 strategies have been adapted previously to understand the governing hydrological processes
42 in the chalk unsaturated zone.

43 In chalk, the matrix provides porosity and storage capacity, while the fractures greatly
44 enhance permeability [Van den Daele *et al.*, 2007]. Water movement through chalk matrix is
45 slow due to its relatively high porosity (0.3-0.4) and low permeability (10^{-9} - 10^{-8} ms $^{-1}$). A
46 fractured chalk system, in contrast, conducts water at a considerably higher velocity because
47 of relatively high permeability (10^{-5} - 10^{-3} ms $^{-1}$) and low porosity (of the order 10^{-4}) of
48 fractures [Price *et al.*, 1993].

49 Simulating water flow through the matrix-fracture system of chalk has been the subject of
50 research for some time. Both conceptual [e.g., *Price et al.*, 2000; *Haria et al.*, 2003] and
51 physics-based [e.g., *Mathias et al.*, 2006; *Ireson et al.*, 2009] models have been proposed
52 previously to describe water flow through chalk unsaturated zone. The physics-based models
53 mentioned above were developed based on dual-continua approach and required relatively
54 large numbers of parameters (*i.e., on the order of 20-30 parameters*) that were calibrated via
55 inverse modelling using observed soil moisture and matric potential data [*e.g., Ireson et al.*,
56 [2009; Mathias et al., 2006](#)].

57 In recent years, representation of chalk has gained attention in land surface modelling. For
58 example, *Gascoin et al.* [2009] applied the Catchment Land Surface Model (CLSM) over the
59 Somme River basin in northern France. A linear reservoir was included in the TOPMODEL
60 based runoff formulation of CLSM to account for the contribution of chalk aquifers to river
61 discharge. *Le Vine et al.* [2016] applied the Joint UK Land Environment Simulator (JULES
62 [*Best et al.*, 2011]) over the Kennet catchment in southern England to evaluate the
63 hydrological limitations of land surface models. In that study, two intersecting Brooks and
64 Corey curves were proposed, which allowed a dual curve soil moisture retention
65 representation for the two distinct flow domains of chalk (*i.e., matrix and fracture*) in the
66 model. Considering this dual Brooks and Corey curve, a three-dimensional groundwater flow
67 model (ZOOMQ3D [*Jackson and Spink*, 2004]) was coupled to JULES to demonstrate the
68 strong influence of representing chalk hydrology and groundwater dynamics on simulated
69 soil moisture and runoff.

70 The above mentioned studies illustrate the importance of representing chalk in land surface
71 modelling. However, including chalk hydrology in large-scale land surface modelling using
72 the contemporary dual-porosity concept can be complicated due to because this approach
73 generally involves relatively large numbers of additional parameters. In this context, we

74 propose a new parameterization, namely the Bulk Conductivity (BC) model as a first step
 75 towards a simple chalk representation suitable for land surface modelling. In order to test the
 76 proposed parameterization, the The BC model is included in JULES (version 4.2), which, by
 77 default (i.e., uniform soil column representation using general soil database as typically
 78 applied in land surface models), does not represent any chalk feature. In this study, the BC
 79 model (included in JULES) is and applied evaluated at two distinct spatial scales (i.e., point
 80 and catchment). At the point-scale, the proposed BC model parameterization is calibrated
 81 evaluated using observed soil moisture profile data. This is achieved by randomly sampling
 82 the parameter space and extensively running the model in order to minimize the differences
 83 between observed and simulated soil moisture variability at different depths. Finally, the The
 84 proposed model is then applied to the Kennet catchment in the Southern England and the
 85 fluxes and states of the hydrological cycle are simulated for multiple years. The simulation
 86 results are evaluated using observed latent heat flux (LE) and runoff data to assess the
 87 performance of the BC model in simulating land surface processes at the catchment scale.

88 2. A model of flow through chalk unsaturated zone

89 In this study, the *Bulk Conductivity* (BC) model based on the work by Zehe *et al.* [2001] is
 90 incorporated in JULES to represent the flow of water through the fractured chalk unsaturated
 91 zone. According to this approach, if the relative saturation (S) exceeds a certain threshold (S_0)
 92 at a soil grid, the saturated hydraulic conductivity of chalk matrix (K_s) is increased to a bulk
 93 saturated hydraulic conductivity (K_{sb}) as follows

$$94 \quad K_{sb} = K_s + K_s f_m \frac{S-S_0}{1-S_0} \quad \text{if } S > S_0 \quad (1)$$

$$95 \quad K_{sb} = K_s \quad \text{if } S \leq S_0 \quad (2)$$

$$96 \quad \text{with } S = \frac{\theta - \theta_r}{\theta_s - \theta_r}$$

97 where f_m is a macroporosity factor (-), θ is soil moisture (m^3m^{-3}), θ_s is soil moisture at
98 saturation (m^3m^{-3}), and θ_r is the residual soil moisture (m^3m^{-3}). Note that S ranges from zero
99 in case of completely dry soils to one for fully wet soils.

100 At the first step of evaluation, the K_s , S_0 and f_m parameters are estimated based on existing
101 literature to assess the performance of the uncalibrated BC model. ~~In this uncalibrated BC~~
102 ~~model, K_s for chalk matrix is 16 mmd^{-1} according to Le Vine et al. [2016] for the catchment~~
103 ~~investigated in this study (Figure 1)~~ For the matrix saturated hydraulic conductivity (K_s), we
104 ~~use $K_s = 1.0 \text{ mmd}^{-1}$ following Mathias et al. [2006]~~. In addition, Equation 1 indicates that the
105 onset of water flow through the fracture system of chalk is controlled by the threshold S_0 .
106 According to Wellings and Bell [1980], water flow through fractures dominates over matrix
107 flow in chalk when the pressure head in soil becomes higher than $-0.50 \text{ mH}_2\text{O}$. We consider a
108 value of $S_0 = 0.80$ for the uncalibrated BC model, which is based on observed soil moisture-
109 matric potential relationship in the study area (Figure S1).

110 Finally, In Zehe et al. [2001], f_m was defined as the ratio of the saturated water flow rate in all
111 macropores in a model element to the corresponding value in soil matrix, which can be
112 determined based on the density and length of fractures at small scales. In addition, f_m has
113 also been considered as a calibration parameter previously [e.g., Blume, 2008; Zehe et al.,
114 2013]. In this study, we define f_m as a characteristic soil property reflecting the influence of
115 fractures on soil water movement [Zehe and Blöschl, 2004], and estimate it from the relative
116 difference of permeability between chalk matrix and fractured chalk system that can be of the
117 order 10^4 - 10^6 according to Price et al. [199³⁹]. Consequently, we consider a macroporosity
118 factor of $f_m = 10^5$ for the uncalibrated BC model. In the following step, the BC model is
119 calibrated to minimize the differences between the variability of observed and simulated soil
120 moisture at individual depths. The calibration strategy will be discussed elaborately in section
121 3.5.

122 In the following step, the BC model parameters are optimized to minimize the differences
 123 between the variability of observed and simulated soil moisture. Price et al. [1999] argued
 124 that the K_s for chalk matrix is generally around $3\text{--}5 \text{ mmd}^{-1}$ ($3.5\text{--}5.8 \times 10^{-5} \text{ mms}^{-1}$). In order to
 125 optimize the BC model performance, we consider a range of $K_s = 0.8\text{--}86 \text{ mmd}^{-1}$ ($10^{-5}\text{--}10^{-3}$
 126 mms^{-1}) for chalk matrix in this study. As mentioned earlier, S is zero for completely dry soils
 127 and one in case of fully wet soils. Therefore, we consider a range of 0–1.0 for S_θ to optimize
 128 the BC model. For f_m , a range of $10^4\text{--}10^6$ is considered, which, as discussed earlier, is
 129 consistent with the relative difference between the permeability of fractured chalk and chalk
 130 matrix according to Price et al [1999].

131 We use the Root Mean Squared Error (RMSE) as the objective function to optimize the BC
 132 model parameters [e.g., Ireson et al., 2009]

$$133 \text{RMSE} = \frac{1}{nd} \sum_{d=1}^{nd} \sqrt{\left(\frac{1}{nt} \sum_{t=1}^{nt} (\Delta\theta_{d,t}^{obs} - \Delta\theta_{d,t}^{sim})^2 \right)} \quad (2)$$

134 where nd is the number of soil layers, nt is the number of soil moisture observations available
 135 for a layer d , $\Delta\theta^{obs}$ is the observed variability of soil moisture and $\Delta\theta^{sim}$ is the simulated
 136 variability of soil moisture. Note that we consider $\Delta\theta$ for this optimization because of its
 137 relevance to the water flux and recharge through chalk unsaturated zone [e.g., Ireson and
 138 Butler, 2011]. Latin hypercube technique [e.g., McKay et al., 2016] is used to generate 2000
 139 random samples for each BC model parameter within the respective range discussed above.
 140 We perform simulations using these random samples and calculate model performance
 141 (Equation 2) to select the optimum parameter values for the BC model (discussed in section
 142 4.1).

143 3. Methods

144 3.1. Study area

145 The study area encompasses the Kennet catchment located in the Southern England with an
146 area of about 1033 km² (Figure 1a). Generally, Kennet is rural in nature with scattered
147 settlements and has a maximum altitude of approximately 297 m (Above Ordnance Level).
148 The River Kennet discharges into the North Sea through London. The major tributaries of
149 this river are Lambourn, Dun, Enborne, and Foudry Brook. An average annual rainfall of
150 approximately 760 mm was recorded in the catchment over a 40 year period from 1961-1990.
151 Solid geology of the Kennet catchment is dominated by chalk, which is overlain by thin soil
152 layer. While lower chalk outcrops along the northern catchment boundary, progressively
153 younger rocks are found in the southern part. In general, surface runoff production is very
154 limited over the regions of the catchment where chalk outcrops. The flow regime shows a
155 distinct characteristics of slow response to groundwater held within the chalk aquifer [*Le*
156 *Vine et al.*, 2016]. According to *Ireson and Butler* [2013], the unsaturated zone of chalk
157 shows slow drainage over summer and bypass flow during wet periods in this catchment.

158 **3.2. Field measurements and remotely sensed data**

159 Table 1 summarizes the field measurements and remote sensing data used in this study. We
160 use *in-situ* soil moisture and runoff measurements along with remotely sensed LE data to
161 assess model performance in simulating the mass and energy balance components of the
162 hydrological cycle. Point scale soil moisture measurements at two adjacent sites (~20 m
163 apart) at the Warren Farm (Figure 1) were provided by Centre for Ecology and Hydrology
164 (CEH). A Didcot neutron probe was used at these locations to measure fortnightly soil
165 moisture at different depths below land surface (10 cm apart down to 0.8 m, 20 cm apart
166 between 0.8-2.2 m, and 30 cm apart between 2.2-4.0 m) [*Hewitt et al.*, 2010].
167 The National River Flow Archive (NRFA) coordinates discharge measurements from the
168 gauging station networks across UK. These networks are operated by the Environmental

169 Agency (England), Natural Resources Wales, Scottish Environment Protection Agency, and
170 Rivers Agency (Northern Ireland). We use discharge measurementss provided by NRFA to
171 calculate the runoff ratio over the Kennet catchment in this study assess model performance
172 in simulating runoff over the Kennet catchment in this study.

173 The MOD16 product of the Moderate Resolution Imaging Spectroradiometer (MODIS) is a
174 part of NASA/EOS project that provides estimation of global terrestrial LE. The LE
175 estimation from MOD16 is based on remotely sensed land surface data [e.g., *Mu et al.*, 2007].
176 In this study, the 8-day and monthly LE data products from MODIS is used to evaluate the
177 model performance in simulating land surface energy fluxes.

178 **3.3. Land surface model**

179 In this study, we use the Joint UK Land Environment Simulator (JULES [e.g., *Best et al.*,
180 2011; *Clark et al.*, 2011]) version 4.2. JULES is a flexible modelling platform with a modular
181 structure aligned to various physical processes developed based on the Met Office Surface
182 Exchange Scheme (MOSES [e.g., *Cox et al.*, 1999; *Essery et al.*, 2003]). Meteorological data
183 including precipitation, incoming short- and longwave radiation, temperature, specific
184 humidity, surface pressure, and wind speed are required to drive JULES. Each grid box in
185 JULES can comprise nine surface types (broadleaf trees, needle leaf trees, C3 grass, C4 grass,
186 shrubs, inland water, bare soil, and ice) represented by respective fractional coverage. Each
187 surface type is represented by a tile and a separate energy balance is calculated for each tile.
188 Subsurface heat and water transport equations are solved based on finite difference
189 approximation in JULES as described in *Cox et al.* [1999]. Moisture transport in the
190 subsurface is described by the finite difference form of Richards' equation. The vertical soil
191 moisture flux is calculated using the Darcy's law. While the top boundary condition to solve

192 the Richards' equation is infiltration at soil surface, the bottom boundary condition in JULES
193 is free drainage that contributes to subsurface runoff.

194 Surface runoff is calculated by combining the equations of throughfall and grid box average
195 infiltration in JULES. In order to direct the generated runoff to a channel network, river
196 routing is implemented based on the discrete approximation of one-dimensional kinematic
197 wave equation [e.g., *Bell et al.*, 2007]. In this approach, river network is derived from the
198 digital elevation model (DEM) of the study area and different wave speeds are applied to
199 surface and subsurface runoff components and channel flows [e.g., *Bell and Moore*, 1998]. A
200 return flow term accounts for the transfer of water between subsurface and land surface [e.g.,
201 *Dadson et al.*, 2010, 2011].

202 **3.4. Model configurations and input data**

203 In this study, simulations are performed at two distinct spatial scales, namely point and
204 catchment. At the point scale, JULES is configured to simulate the mass and energy fluxes at
205 the Warren Farm site (Figure 1a). A total subsurface depth of 5 m is considered in the model
206 with a vertical discretization ranging from 10 cm at the land surface to 50 cm at the bottom of
207 the model domain. Note that this discretization is consistent with the soil moisture
208 measurement depths mentioned in section 3.2. The vegetation type is implemented as C3
209 grass using the default parameters in JULES. Point scale simulations were performed over 2
210 consecutive years from 2003-2005 at an hourly time step. Except for precipitation, hourly
211 atmospheric forcing data to drive JULES was obtained from an automatic weather station
212 operated by the CEH at Warren Farm. In order to estimate hourly precipitation data to run
213 JULES, rain gauge measurements from the Met Office [*Met Office*, 2006] were used. Inverse
214 distance interpolation technique [e.g. *Garcia et al.*, 2008; *Ly et al.*, 2013] was applied on

215 rainfall measurements from 13 gauges closest to Warren Farm (distance varies from 25-60
216 km) to obtain hourly precipitation for the point scale simulations.

217 At the catchment scale, JULES is configured over a study area encompassing the Kennet
218 catchment (Figure 1a) considering a uniform lateral grid resolution of 1 km with 70 x 40 cells
219 in x and y dimensions, respectively. The total subsurface depth and vertical discretization are
220 identical to those of the point scale simulations. Spatially distributed vegetation type
221 information for the study area (Figure 1b) is obtained from the Land Cover Map 2007
222 (LCM2007) dataset [Morton *et al.*, 2011]. Simulations were performed over 5 consecutive
223 years from 2006-2011 at the catchment scale. Note that the simulation periods of catchment
224 and point scale (2003-2005) does not coincide due to the availability of soil moisture
225 measurements described in section 3.2. Spatially distributed meteorological data from the
226 Climate, Hydrology and Ecology research Support System (CHESS) was used to obtain the
227 atmospheric forcing to drive JULES at the catchment scale. The CHESS data includes 1 km
228 resolution gridded daily meteorological variables [Robinson *et al.*, 2015]. This daily data is
229 downscaled using a disaggregation technique described in Williams and Clark [2014] to
230 obtain hourly atmospheric forcing. The flow direction required for river routing is extracted
231 from the USGS HydroSHEDS digital elevation data [Lehner *et al.*, 2008].

232 We estimate the soil hydraulic properties based on texture (Table 2). At the point scale, loam
233 soil is dominant at the Warren Farm site. At the catchment scale, the Harmonized World Soil
234 Database (HWSD) from the Food and Agricultural Organization of UNO (FAO) is used to
235 obtain the texture of different soil types over Kennet (Figure 1c). The saturation-pressure
236 head relationship for different soil types is described using the Van Genuchten [Van
237 Genuchten, 1980] model with parameter values (Table 2) obtained from Schaap and Leij
238 [1998].

239 [Table 3 summarizes](#) The hydraulic properties for chalk used in this study [are summarized in](#)
240 [Table 3](#). These properties are obtained based on existing literature as a first step when
241 evaluating the uncalibrated BC model. The BC model parameters are subsequently [optimized](#)
242 [calibrated](#) to minimize the differences between observed and simulated $\Delta\theta$ [\(section 3.5\)](#) at
243 [various soil depths](#).

244 In this study, we consider two different model configurations, namely *default* and *macro*
245 (Figure 2). The *default* configuration corresponds to the standard parameterizations of JULES
246 that does not represent chalk hydrology in the model. In this configuration, each soil column
247 in JULES is considered to be vertically homogeneous with the soil properties defined in
248 Table 2, which is motivated by the Met Office JULES Global Land 4.0 configuration
249 described in *Walters et al. [2014]*. The *macro* configuration, in contrast, explicitly represents
250 chalk by applying the BC model starting at 30 cm below land surface to the bottom of the
251 model domain (i.e. 500 cm). Therefore, the soil column in the *macro* configuration can be
252 divided into topsoil (0-30 cm) and chalk (30-500 cm) [in *macro*](#). The topsoil depth of 30 cm [in](#)
253 [the *macro* configuration](#) is defined based on several augured soil samples collected during a
254 field campaign at Warren Farm in 2015 (Figure 2). This depth is corroborated by additional
255 information from the British Geological Survey (BGS) operated borehole records
256 (http://www.ukso.org/pmm/soil_depth_samples_points.html), which show that topsoil depths
257 vary from 10-40 cm over the study area. We [therefore](#) apply the *macro* configuration
258 assuming a spatially homogeneous topsoil depth of 30 cm for both point and catchment scale
259 simulations. Note that except for this inclusion of chalk, *default* and *macro* configurations are
260 identical in terms of model set up and input data. [It should also be emphasized that *default*](#)
261 [represents a “naïve” configuration deprived of model calibration. Moreover, this](#)
262 [configuration does not represent chalk, which, according to previous studies \[e.g., *Le Vine et*](#)
263 [al., 2016\], substantially affects the hydrology of the study area considered here.](#)

264 3.5. Calibration of the BC model

265 We calibrate the BC model at the point-scale to minimize the differences between observed
266 and simulated soil moisture variability ($\Delta\theta$) at different depths. The Root Mean Squared
267 Error (RMSE) is used as the objective function to optimize the BC model parameters [e.g.,
268 *Ireson et al., 2009*]

269
$$RMSE = \frac{1}{nd} \sum_1^{nd} \sqrt{\left(\frac{1}{nt-1} \sum_2^{nt} (\Delta\theta_{d,t}^{obs} - \Delta\theta_{d,t}^{sim})^2 \right)} \quad (3)$$

270 where nd is the number of soil layers, nt is the number of soil moisture observations available
271 for a layer d , $\Delta\theta^{obs}$ is the observed variability of soil moisture and $\Delta\theta^{sim}$ is the simulated
272 variability of soil moisture. Note that we consider $\Delta\theta$ for this optimization because of its
273 relevance to the water flux and recharge through chalk unsaturated zone [e.g., *Ireson and*
274 *Butler, 2011*].

275 Equation (1) reveals that the calibration of the BC model involves optimizing 3 parameters,
276 namely the saturated hydraulic conductivity of chalk matrix (K_s), saturation threshold (S_0)
277 and macroporosity factor (f_m). *Ireson et al.* [2009] suggested a range of 0.2-2.0 m m^{-1} for K_s .
278 On the other hand, *Price et al.* [1993] argued that in general, K_s is around 3-5 m m^{-1} for most
279 chalk soils. Therefore, we consider a range of 0.2-5.0 m m^{-1} in optimizing K_s . We consider S_0
280 range 0-1, representing the entire physical domain for soil wetness from fully dry to fully
281 wet, respectively. As mentioned earlier, S_0 is zero for completely dry soils and one in case of
282 fully wet soils. Consequently, we consider $S_0 = 0.0-1.0$ in the optimization. For f_m , a range of
283 10^4-10^6 is considered, which, as discussed earlier, is consistent with the relative difference
284 between the permeability of fractured chalk and chalk matrix according to *Price et al* [1993].
285 Latin hypercube sampling technique [e.g., *McKay et al.*, 2016] is used to generate 2,000
286 random samples for each BC model parameter within the ranges discussed above. Note that
287 for the K_s parameter, the random sampling was performed from a logarithmic distribution

288 [Ireson et al., 2009]. We perform simulations using these random samples and calculate
289 model performance (Equation 3) to select the optimum parameter values for the BC model
290 for each possible parameter combination as discussed in details in the following section.

291 4. Results and discussion

292 4.1. Point scale simulations

293 At the point scale, the simulation results are evaluated using soil moisture observations at the
294 Warren Farm site. Figure 3a compares observed and simulated soil moisture (θ) from the
295 *default* and *macro* configurations at 2 m below land surface. Note that the *macro*
296 configuration uses the chalk hydraulic parameters collected from existing literature (Table 3).
297 This figure shows that the *default* configuration considerably underestimates θ throughout the
298 simulation period, which is improved remarkably in case of *macro*. Figure 3b plots observed
299 and simulated soil moisture variability ($\Delta\theta$) from the *default* and *macro* configurations
300 ($\Delta\theta_{\text{default}}$ and $\Delta\theta_{\text{macro}}$, respectively) at the Warren Farm site. In general, both configurations
301 show discrepancies with observed $\Delta\theta$ with *macro* showing relatively better model
302 performance.

303 The results show that despite the *macro* configuration improves simulated θ , it shows
304 considerable discrepancies with observed $\Delta\theta$, which is consistent throughout the whole chalk
305 profile (results from other model layers are not shown). In order to minimize the differences
306 between observed and modelled $\Delta\theta$ from the *macro* configuration, we calibrate optimize the
307 BC model following the methodology described in section [3.52](#). The optimization results are
308 summarized in Figure 4. Note that for each combination considered in the optimization, 2,000
309 model runs were performed using randomly sampled parameters as discussed in section [3.52](#).
310 In addition to the *default* and *macro* cases, the calibrated cases in Figure 4 presents

311 correspond to the results from the model runs yielding the lowest RMSE for each parameter
312 combination evaluated.

313 The RMSE between observed and simulated $\Delta\theta$ for the model configurations considered in
314 the optimization is shown in Figure 4a. This figure illustrates that the RMSE of the *default*
315 configuration is larger than that of *macro*, indicating better model performance in
316 reproducing $\Delta\theta$ for the latter (corresponding to a reduction of 15% in RMSE compared to the
317 *default case*). Therefore, it appears that the uncalibrated BC model (i.e., the *macro*
318 configuration) is better in reproducing reproduces the soil moisture variability compared to
319 *default*. Figure 4b, c and d presents the BC model parameter values from the model run
320 producing the lowest RMSE for each configuration. Concerning the calibration of single BC
321 model parameters, Figure 4a shows that optimizing S_0 results in a 46% 16% reduction of
322 RMSE compared to the *macro* configuration. Calibrating Optimizing K_s marginally improves
323 model performance, which is observed from a slightly lower (4%) RMSE than *macro* or f_m
324 individually yields only about 25% reduction of RMSE compared to *macro*.

325 Optimizing both K_s and S_0 simultaneously shows results in the largest reduction (5024%) of
326 RMSE compared to *macro* which coincides with the total RMSE reduction found when all
327 parameters are calibrated. Arguably, the BC model can be implemented in other chalk
328 regions by constraining only S_0 parameter. Such result could potentially be advantageous for
329 transferability to other regions in the UK in order to assess chalk hydrology at large-scale.
330 However since this is the first time the BC model is introduced, we decide to take a
331 conservative approach and select the *macro* configuration with optimized K_s and S_0 ($macro_{opt}$)
332 hereafter) to simulate chalk hydrology over the study area that ensures best overall model
333 performance.

334 The lower three panels in Figure 4 presents the BC model parameter values for the *default*
335 and uncalibrated *macro* cases as well as for different combinations of parameters calibrated.
336 The red bars in Figure 4a, b and c highlight the cases in which a given parameter is
337 constrained by optimization. In those cases, the calibrated parameter values are obtained from
338 model runs producing the lowest RMSE. An interesting feature in Figure 4b (calibrating K_s
339 individually) is that the optimization suggests a compensation mechanism in which K_s is
340 increased remarkably in order to physically represent the “effective” flow through the chalk
341 fractures in the BC model. This is not surprising and arguably the simplest way to attempt to
342 improve model performance. For $macro_{opt}$, the values used for K_s is relatively lower than that
343 of uncalibrated *macro* case nevertheless consistent with previous estimates [e.g., Ireson *et al.*,
344 2009]. Figure 4c clearly shows the dominance of S_0 in the BC model as all the relatively low
345 RMSE bars in Figure 4a are associated with S_0 calibration (see red bars in Figure 4c). In
346 addition, calibrated S_0 values for all cases show a consistent constraint around 0.50. Finally,
347 Figure 4d indicates the lack of influence for f_m parameter on model performance.
348 Additionally, Figure 4 suggests that the sensitivity of S_0 on the model performance in
349 simulating $\Delta\theta$ is substantially higher compared to K_s and f_m , which is corroborated by the
350 sensitivity of the individual model parameters (Figure S2). Figure 4a also reveals the
351 interesting fact that the RMSE from the configuration with optimized K_s and S_0 is identical to
352 that of the one with all 3 parameters optimized simultaneously (i.e., K_s , S_0 and f_m). Therefore,
353 we select the *macro* configuration with optimized K_s and S_0 ($macro_{opt}$ hereafter) to simulate
354 chalk hydrology over the study area.

355 Figure 5 compares $\Delta\theta_{default}$, $\Delta\theta_{macro}$ and $\Delta\theta$ from the $macro_{opt}$ configuration ($\Delta\theta_{opt}$) with
356 observed soil moisture variability ($\Delta\theta_{obs}$). As mentioned earlier, $\Delta\theta_{default}$ and $\Delta\theta_{macro}$ show
357 considerable discrepancies with $\Delta\theta_{obs}$ while the *macro* configuration exhibits relatively better
358 performance (Figure 3). Figure 5 illustrates that the overall agreement between observed and

359 simulated $\Delta\theta$ improves substantially in case of $macro_{opt}$ compared to $default$ and $macro$,
360 which is pronounced especially in the deeper chalk layers. Therefore, this figure indicates
361 that the performance of the BC model in simulating $\Delta\theta$ is further improved by optimizing the
362 K_s and S_0 parameters simultaneously at the Warren Farm site.

363 In order to assess the model performance in simulating soil moisture over the entire column,
364 the relative bias ($\Delta\mu$, see Appendix) of simulated θ from the $default$ and $macro_{opt}$
365 configurations at Warren Farm for various depth ranges are shown in Figure 6. In the soil
366 layers (0–30 cm), θ from the two configurations are comparable with the $default$ showing
367 slightly lower mean relative bias ($\Delta\mu_{mean}$) of 0.03 than $macro_{opt}$ ($\Delta\mu_{mean} = 0.12$ –0.09).
368 However, in the chalk layers (30–500 cm), $default$ simulates substantially drier conditions,
369 corresponding to $\Delta\mu_{mean} \leq 0.28$. In contrast, the $macro_{opt}$ configuration considerably
370 improves the agreement between the simulated and observed θ in the chalk layers with $\Delta\mu_{mean}$
371 $\Delta\mu_{mean} \geq 0.24$ –0.05. Therefore, the results indicate that the inclusion of the BC model in
372 JULES improves the performance of overall soil moisture simulation (both θ and $\Delta\theta$) at
373 Warren Farm especially in the chalk layers although underestimation of θ compared to
374 measurements was observed for both $default$ and $macro_{opt}$ configurations.

375 As mentioned earlier, efficiently reproducing soil moisture variability over the profile is
376 important due to the fact that $\Delta\theta$ significantly affects water flux and recharge through chalk
377 unsaturated zone. The drainage flux through the bottom of soil column (d_b) of a land surface
378 model can be considered as the potential recharge flux to groundwater [e.g., Sorensen *et al.*,
379 2014]. Figure 7–6 compares the daily sum of d_b from the $default$ and $macro_{opt}$ configurations
380 at the Warren Farm site. Daily The rainfall at this site characteristics over the simulation
381 study period is shown in Figure 7a–6a. In Figure 7–6b, the $macro_{opt}$ configuration shows
382 considerable d_b during the colder months, while relatively slow drainage is observed in
383 summer prevails throughout the rest of the year. In contrast, the $default$ configuration shows

384 relatively high d_b in summer compared to the colder months. In general, the recharge rate
385 through chalk unsaturated zone during the warmer periods of the year is lower than that in the
386 winter months [Wellings and Bell, 1980; Ireson et al., 2009]. Therefore, the $macro_{opt}$
387 configuration appears to be more consistent with the recharge mechanism in chalk compared
388 to *default*.

389 In this section, the BC model was evaluated at the point scale. The results showed that in
390 general, the *macro* configuration outperforms the *default* case relatively better in in
391 simulating θ and $\Delta\theta$ compared to *default*. In order to improve the model performance even
392 further, model parameter calibration parameter optimization was performed to minimize the
393 differences between observed and simulated $\Delta\theta$ at the point scale. In the next sections, the
394 optimized model ($macro_{opt}$) is evaluated at the catchment scale.

395 **4.2. Catchment scale simulations**

396 In the previous section, it was observed that the *default* configuration generally
397 underestimates θ compared to $macro_{opt}$. Previous studies have demonstrated the
398 interconnections between shallow soil moisture and LE [e.g., Chen and Hu, 2004]. At the
399 catchment scale, simulation results from the *default* and $macro_{opt}$ configurations are
400 compared with the observations over the Kennet catchment. In order to assess the differences
401 between the LE from the *default* and $macro_{opt}$ configurations at the catchment scale, Figure 8
402 7 plots spatially averaged 8-day composites of LE from MODIS (LE_{MOD}) against the LE from
403 these configurations ($LE_{default}$ and LE_{opt} , respectively) over Kennet. The agreement between
404 simulated LE and LE_{MOD} is evaluated using the coefficient of determination (R^2 , see
405 Appendix) and mean bias. Comparison between $LE_{default}$ and LE_{MOD} shows a coefficient of
406 determination of $R^2_{default} = 0.78$ and a mean bias of $bias_{default} = 10.5 \text{ Wm}^{-2}$. The agreement
407 between simulated LE and LE_{MOD} improves in case of the $macro_{opt}$ configuration, which is

408 reflected by an increased coefficient of determination of $R^2_{opt} = 0.800.81$ and a reduced mean
409 bias of $bias_{opt} = 7.13 \text{ Wm}^{-2}$.

410 Figure 78 shows considerable differences between $LE_{default}$ and LE_{opt} especially for relatively
411 high LE, indicating discrepancies especially during the warmer months of the year. Figure 9a
412 presents ~~s~~ Spatially averaged time series of monthly LE_{MOD} , $LE_{default}$ and LE_{opt} is presented in
413 Figure 8a. - This figure shows that the differences between $LE_{default}$ and LE_{opt} increases
414 substantially in summer compared to the colder months of the year, which is consistent with
415 Figure 87. Consequently, the *default* configuration underestimates LE in summer compared
416 to LE_{MOD} , which is improved in case of the $macro_{opt}$ configuration. In contrast, the
417 differences between $LE_{default}$ and LE_{opt} are negligible during the colder months of the year.

418 In addition, Figure 98b compares the observed and simulated monthly average discharge
419 from the two model configurations at the “Kennet at Theale” gauging station (Figure 1a).
420 This figure depicts that the *default* configuration generally overestimates discharge at this
421 gauging station, which is improved considerably in the case of $macro_{opt}$. We use the Kling-
422 Gupta Efficiency criteriaon (KGE [Gupta *et al.*, 2009]) to compare the performance of the
423 two model configurations in reproducing observed discharge variability. As mentioned
424 above, the *default* configuration overestimates discharge with $KGE_{default} = -0.17$. On the other
425 hand, the $macro_{opt}$ configuration improves the agreement between observed and simulated
426 discharge, which is reflected by $KGE_{opt} = 0.51$.

427 In order to summarize the results at catchment scale, Table 4 compares observed and
428 simulated daily average runoff from the two model configurations over the Kennet catchment
429 from 2006-2011. The runoff ratio (*RR*, see Appendix), which is equal to the mean volume of
430 flow divided by the volume of precipitation [e.g., Kelleher *et al.*, 2015], assesses the
431 partitioning of precipitation into runoff over the catchment. The *default* configuration (*RR* =

432 0.82) shows considerably higher RR compared to observation ($RR = 0.40$), indicating
433 overestimation of runoff by the model [that is consistent with Figure 98b](#). Including chalk
434 hydrology in the model remarkably improves the agreement between observed and simulated
435 mean runoff over the Kennet catchment, which is assessed from a runoff ratio of $RR = \underline{0.46}$
436 [0.37](#) for the $macro_{opt}$ configuration [which is much closer to the observed RR value than](#)
437 [default](#).

438 In Table 4, the relative bias ($\Delta\mu$) of 1.04 between observed and simulated runoff from the
439 *default* configuration again indicates the overestimation by the model. In comparison,
440 $macro_{opt}$ shows a [smaller](#) relative bias [of](#) $\Delta\mu = \underline{0.12-0.05}$, indicating [improved](#) [agreement](#) between observed and simulated mean runoff volume compared to *default*. The
441 [agreement](#) between observed and simulated mean runoff volume compared to *default*. The
442 relative difference in standard deviation ($\Delta\sigma$, see Appendix) compares the variability of
443 observed and simulated [flow runoff](#) in Table 4 [relating directly to the seasonal change in](#)
444 [runoff](#). This comparison shows that the *default* configuration overestimates the variability of
445 runoff over the Kennet catchment ($\Delta\sigma = 2.04$), which is improved in case of $macro$ ($\Delta\sigma =$
446 [0.650.70](#)). [This improvement in reproducing flow variability is also clearly observed in](#)
447 [Figure 8b](#).

448 [It was demonstrated previously that the *default* configuration predicts lower](#)
449 [evapotranspiration \(ET\) compared to \$macro_{opt}\$ over the Kennet catchment due to the](#)
450 [differences in simulated \$\theta\$. In JULES, moisture from soil and canopy is depleted to meet the](#)
451 [ET demand. Additionally, surface runoff generation depends on canopy water storage in the](#)
452 [model \[Best et al., 2011\]. Because of this connection between ET and surface runoff](#)
453 [generation via canopy water storage, the differences in runoff demonstrated in Table 4 can be](#)
454 [attributed to the disagreements between \$LE_{default}\$ and \$LE_{macro}\$ \(Figure 8\) due to the relatively](#)
455 [drier conditions simulated by *default*.](#)

456 In this section, the BC model is evaluated using observed mass and energy fluxes over the
457 Kennet catchment. The *default* configuration ~~showed considerably suggested relatively~~ low
458 ~~summertime~~ LE over the catchment, ~~which was pronounced during the warmer period of the~~
459 ~~year~~. The agreement between observed and simulated LE was improved in case of the
460 *macro_{opt}* configuration compared to *default*. It was also observed that the overall runoff
461 prediction was considerably improved by *macro_{opt}* compared to *default*. Given its simplicity,
462 our results indicate that the proposed parameterization is suitable for use in land surface
463 modelling applications.

464 **5. Summary and Conclusions**

465 In this study, we proposed a simple parameterization, namely the *Bulk Conductivity* (BC)
466 model to simulate water flow through the matrix-fracture system of chalk in large scale land
467 surface modelling applications. This parameterization was implemented in the Joint UK Land
468 Environment Simulator (JULES) and applied to the Kennet catchment located in the southern
469 UK to simulate the mass and energy fluxes of the hydrological cycle for multiple years. Two
470 model configurations, namely *default* and *macro* were considered with the latter using the BC
471 model to simulate chalk hydrology.

472 The proposed BC model is a single continuum approach of modelling preferential flow [e.g.,
473 *Beven and Germann, 2013*] that involves only 32 parameters, namely the saturated hydraulic
474 conductivity of chalk matrix (K_s), macroporosity factor (f_m) and relative saturation threshold
475 (S_0). Initially, these parameters along with the saturated hydraulic conductivity of the chalk
476 matrix were estimated from existing literature to assess the performance of the uncalibrated
477 BC model. Finally, the BC model parameters were optimized to minimize the differences
478 between observed and simulated soil moisture variability. Our results indicated that S_0 is by
479 far the most influential parameter in the model when representing water movement through a

480 soil-chalk column. This highlights the simplicity of the proposed BC model for large-scale
481 studies and potential ease in transferability. followed by In comparison, Parameters K_s the
482 saturated hydraulic conductivity of chalk matrix while and f_m showed secondary (low)
483 sensitivity on the model performance. Since this study introduces the BC model, we decided
484 however to take a conservative approach. Motivated by the sensitivity analysis, we We
485 optimized K_s and S_0 simultaneously for our catchment scale simulations since this
486 combination resulted in the best overall model performance in the next step that considerably
487 improved the agreements between observed and simulated soil moisture variability. Note that
488 calibrating the BC model involves optimizing only 2 out of 3 parameters. This reduced
489 complexity may add considerable benefits in applying the proposed model over large areas.
490 Hence, the parameterization is further improved by optimizing both saturated hydraulic
491 conductivity of chalk matrix and S_0 to minimize the differences between observed and
492 simulated soil moisture variability.

493

494 The simulation results were evaluated using observed mass and energy fluxes both at point
495 and catchment scales. The results demonstrated that the inclusion of the BC model in JULES
496 improves simulated soil moisture variability at the point scale compared to a model
497 configuration that does not represent chalk in the subsurface (i.e., the *default* configuration).
498 At the catchment scale, it was illustrated that the proposed BC parameterization improves
499 simulated latent heat flux (especially in summer) and the overall runoff compared to the
500 default configuration.

501 Note that the complexity (i.e., number of parameters) of the BC model for simulating water
502 flow through chalk unsaturated zone is substantially lower compared to more commonly used
503 models for this purpose (e.g., dual-porosity models). Despite its simplicity, it appears that the

504 proposed parameterization considerably improves the key hydrological mass and energy
505 fluxes simulated by JULES over the Kennet at the catchment-scale. As mentioned
506 previously, representing chalk hydrology in land surface models using the dual porosity
507 concept is complicated mainly due to the relatively large number of parameters involved in
508 such approach. Therefore, the simplified aspect of the BC model parameterization proposed
509 in this study may can potentially be useful for large-scale land surface modelling applications
510 over large-scale chalk-dominated areas.

511 **Acknowledgements**

512 We gratefully acknowledge the support by the “A MUlti-scale Soil moisture
513 Evapotranspiration Dynamics study – AMUSED” project funded by Natural Environment
514 Research Council (NERC) grant number NE/M003086/1. The authors would also like to
515 thank Ned Hewitt and Jonathan Evans from the Centre for Ecology and Hydrology (CEH) for
516 providing the data for the point-scale analyses at the Warren Farm. Finally, wWe would also
517 like to thank Miguel Rico-Ramirez (University of Bristol) for helping preparing the
518 precipitation data from the rain gauge network used for the point-scale simulations, Thorsten
519 Wagener (University of Bristol) for his valuable suggestions on model diagnostics, and Joost
520 Iwema (University of Bristol) for helping with the soil samples collected during the 2015
521 field work campaign. Finally, we would like to thank the reviewers for their comments and
522 suggestions that added to the quality of this manuscript.

523 **Appendix**

524 **Definition of Statistical Metrics**

525 Coefficient of determination (R^2) for observation $y = y_1, \dots, y_n$ and prediction $f = f_1, \dots, f_n$
526 is defined as

527 $R^2 = 1 - \frac{SS_{res}}{SS_{tot}}$

528 where SS_{res} is the residual sum of square and SS_{tot} is the total sum of square. SS_{res} and SS_{tot}
529 are defined as

530 $SS_{res} = \sum_{i=1}^n (y_i - f_i)^2$ and

531 $SS_{tot} = \sum_{i=1}^n (y_i - \bar{y})^2$ with \bar{y} being the mean of y .

532 Runoff ratio (RR) assesses the portion of precipitation that generates runoff over the
533 catchment. RR is defined as

534 $RR = \frac{\mu_{runoff}}{\mu_{rain}}$

535 where μ_{runoff} is mean runoff and μ_{rain} is mean precipitation [e.g., *Kelleher et al.*, 2015].

536 Relative bias ($\Delta\mu$) between observed and simulated time series can be defined as

537 $\Delta\mu = \frac{\mu_{mod} - \mu_{obs}}{\mu_{obs}}$

538 where μ_{obs} and μ_{mod} are the mean of observed and simulated time series, respectively. While
539 the optimal value of $\Delta\mu$ is zero, negative (positive) values indicate an underestimation
540 (overestimation) by the model [e.g., *Gudmundsson et al.*, 2012].

541 Relative difference in standard deviation ($\Delta\sigma$) between observed and simulated time series
542 can be defined as

543 $\Delta\sigma = \frac{\sigma_{mod} - \sigma_{obs}}{\sigma_{obs}}$

544 where σ_{obs} and σ_{mod} are the standard deviation of observed and simulated time series,
545 respectively [e.g., *Gudmundsson et al.*, 2012].

546

547 **References**

548 Bakopoulou, C. (2015), Critical assessment of structure and parameterization of JULES land
549 surface model at different spatial scales in a UK Chalk catchment, PhD thesis, Imperial
550 College London, UK, available at: <https://spiral.imperial.ac.uk:8443/handle/10044/1/28955>.

551 Bell, V. A. and R. J. Moore (1998), A grid-based flood forecasting model for use with
552 weather radar data: Part 1. Formulation, *Hydrol. Earth Syst. Sc.*, 2, 265-281.

553 Bell, V. A., A. L. Key, R. G. Jones, and R. J. Moore (2007), Development of a high
554 resolution grid-based river flow model for use with regional climate model output, *Hydrol.*
555 *Earth Syst. Sc.*, 11, 532-549.

556 Best, M. J., M. Pryor, D. B. Clark, G. G. Rooney, R. I. H. Essery, C. B. Ménard, J. M.
557 Edwards, M. A. Hendry, A. Porson, N. Gedney, L. M. Mercado, S. Sitch, E. Blyth, O.
558 Boucher, P. M. Cox, C. S. B. Grimmond, and R. J. Harding (2011), The Joint UK Land
559 Environment Simulator (JULES), Model Description – Part 1: Energy and Water
560 Fluxes, *Geosci. Model Dev.*, 4, 677-699.

561 Beven, K., and P. Germann (2013), Macropores and water flow in soils revisited, *Water*
562 *Resour. Res.*, 49, 3071–3092.

563 Bloomfield, J. (1997), The role of diagenesis in the hydrogeological stratification of
564 carbonated aquifers: An example from the chalk at Fair Cross, Berkshire, UK, *Hydrol. Earth*
565 *Syst. Sc.*, 1, 19-33.

566 Blume, T. (2008), Hydrological processes in volcanic ash soils: measuring, modelling and
567 understanding runoff generation in an undisturbed catchment, PhD thesis, Institut für

568 Geoökologie, Universität Potsdam, Potsdam, Germany, available at: https://publishup.univ-potsdam.de/opus4-ubp/files/1524/blume_diss.pdf

569

570 Brouyère, S. (2006), Modelling the migration of contaminants through variably saturated

571 dual-porosity, dual-permeability chalk, *J. Contam. Hydrol.*, 82, 195-219.

572 [Chen, X., and Q. Hu \(2004\), Groundwater influences on soil moisture and surface](#)

573 [evaporation, *J. Hydrol.*, 297, 285-300.](#)

574 Clark, D. B., L. M. Mercado, S. Sitch, C. D. Jones, N. Gedney, M. J. Best, M. Pryor, G. G.

575 Rooney, R. L. H. Essery, E. Blyth, O. Boucher, R. J. Harding, C. Huntingford, and P. M. Cox

576 (2011), The Joint UK Land Environment Simulator (JULES), Model Description – Part 2:

577 Carbon Fluxes and Vegetation Dynamics, *Geosci. Model Dev.* 4, 701-722.

578 Cox, P. M., R. A. Betts, C. B. Bunton, R. L. H. Essery, P. R. Rowntree and J. Smith (1999),

579 The impact of new land surface physics on the GCM simulation of climate and climate

580 sensitivity, *Clim. Dynam.*, 15, 183-203.

581 Dadson, S. J., I. Ashpole, P. Harris, H. N. Davies, D. B. Clark, E. Blyth, and C. M. Taylor

582 (2010), Wetland inundation dynamics in a model of land surface climate: Evaluation in the

583 Niger inland delta region, *J. Geophys. Res.*, 115.

584 Dadson, S. J., V. A. Bell, and R. G. Jones (2011), Evaluation of a grid based river flow model

585 configured for use in a regional climate model, *J. Hydrol.*, 411, 238-250.

586 Dettinger, M. D., and H. F. Diaz (2000), Global characteristics of streamflow seasonality and

587 variability, *J. Hydrometeorol.*, 1, 289-310.

588 Essery, R., M. Best, and P. Cox (2001), MOSES 2.2 technical documentation (Hadley Centre

589 technical note 30), Hadley Centre, Met Office, UK.

590 Garcia, M., C. D. Peters-Lidard, and D. C. Goodrich (2008), Spatial interpolation of
591 precipitation in a dense gauge network for monsoon storm events in the southwestern United
592 States, *Water Resour. Res.*, 44.

593 Gascoin, S., A. Duchare, P. Ribstein, M. Carli, and F. Habtes (2000), Adaptation of a
594 catchment-based land surface model to the hydrological setting of the Somme River basin
595 (France), *J. Hydrol.*, 368, 105-116.

596 Gudmundsson, L., T. Wagener, L. M. Tallaksen, and K. Engeland (2012), Evaluation of nine
597 large-scale hydrological models with respect to the seasonal runoff climatology in Europe,
598 *Water Resour. Res.*, 48.

599 Gupta, H. V., H. Kling, K. K. Yilmaz, and G. F. Martinez (2009), Decomposition of the mean
600 squared error and NSE performance criteria: implications for improving hydrological
601 modelling, *J. Hydrol.*, 377, 80-91.

602 Haria, A. H., M. G. Hodnett, and A. C. Johnson (2003), Mechanisms of groundwater
603 recharge and pesticide penetration to chalk aquifer in southern England, *J. Hydrol.*, 275, 122-
604 137.

605 Hartmann, A., N. Goldscheider, T. Wagener, J. Lange, and M. Weiler (2014), Karst water
606 resources in a changing world: Review of hydrological modeling approaches, *Rev. Geophys.*,
607 52, 218–242, doi:10.1002/2013RG000443.

608 Hewitt, N., M. Robinson, and D. McNeil (2010), Pang and Lambourn hydrometric review
609 2009, Wallingford, NERC/Centre for Ecology and Hydrology, (CEH project number:
610 C04076).

611 Ireson, A. M., S. A. Mathias, H. S. Wheater, A. P. Butler and J. Finch (2009), A model for
612 flow in the chalk unsaturated zone incorporating progressive weathering, *J. Hydrol.*, 365,
613 244-260.

614 Ireson, A. M. and A. P. Butler (2011), Controls on preferential recharge to chalk aquifers, *J.*
615 *Hydrol.*, 398, 109-123.

616 Ireson, A. M. and A. P. Butler (2013), A critical assessment of simple recharge models:
617 application to the UK chalk, *Hydrol. Earth Syst. Sc.*, 17, 2083-2096.

618 Ireson, A. M., H. S. Wheater, A. P. Butler, S. A. Mathias, J. Finch, and J. D. Cooper (2006),
619 Hydrological processes in the chalk unsaturated zone – insight from an intensive field
620 monitoring program, *J. Hydrol.*, 330, 29-43.

621 Ireson, A. M., S. A. Mathias, H. S. Wheater, A. P. Butler, and J. Finch (2009), A model for
622 flow in the chalk unsaturated zone incorporating progressive weathering, *J. Hydrol.*, 365,
623 244-260.

624 Jackson, C. and Spink, A. (2004) User's Manual for the Groundwater Flow Model
625 ZOOMQ3D, IR/04/140, British Geological Survey, Nottingham, UK.

626 Kelleher, C., T. Wagener, and B. McGlynn (2015), Model-based analysis of the influence of
627 catchment properties on hydrologic partitioning across five mountain headwater
628 subcatchments, *Water Resour. Res.*, 51, 4109-4136.

629 Kling, H., M. Fuchs, and M. Paulin (2012), Runoff conditions in the upper Danube basin
630 under an ensemble of climate change scenarios. *Journal of Hydrology*, Volumes 424-425, 6
631 March 2012, 264-277.

632 Lehner, B., K. Verdin, and A. Jarvis (2008), New global hydrography derives from
633 spaceborne elevation data, EOS, Transactions, AGU, 89(10), 93-94.

634 Le Vine, N., A. Butler, N. McIntyre, and C. Jackson (2016), Diagnosing hydrological
635 limitations of a land surface model: application of JULES to a deep-groundwater chalk basin,
636 Hydrol. Earth Syst. Sc., 20, 143-159.

637 Lee, L. J. E., D. S. L. Lawrence, and M. Price (2006), Analysis of water-level response to
638 rainfall and implications for recharge pathways in the chalk aquifer, SE England, J. Hydrol.,
639 330, 604-620.

640 Ly, S., C. Charles, and A. Degré (2013), Different methods for spatial interpolation of rainfall
641 data for operational hydrology and hydrological modeling at watershed scale. A review,
642 Biotechnol. Agron. Soc. Environ. 17, 392-406.

643 Mathias, S. A., A. P. Butler, B. M. Jackson, and H. S. Wheater (2006), Transient simulations
644 of flow and transport in the chalk unsaturated zone, J. Hydrol., 330, 10-28.

645 Met Office (2006), UK hourly rainfall data, Part of the Met Office Integrated Data Archive
646 System (MIDAS), NCAS British Atmospheric Data Centre, 21 March 2016,
647 <http://catalogue.ceda.ac.uk/uuid/bbd6916225e7475514e17fdbf11141c1>.

648 Morton, D., C. Rowland, C. wood, L. Meek, C. Marston, G. Smith, R. Wadsworth, and I. C.
649 Simpson (2011), Final report for LCM2007 – the new UK Land Cover Map (CS technical
650 report no 11/07), Centre for Ecology and Hydrology, UK.

651 Mu, Q., F. A. Heinsch, M. Zhao, and S. W. Running (2007), Development of a global
652 evapotranspiration algorithm based on MODIS and global meteorology data, Remote Sens.
653 Environ., 111, 519-536.

654 Price, A., R. A. Downing, and W.M. Edmunds (1993), The chalk as an aquifer. In: Downing,
655 R. A., M. Price, and G. P. Jones *The hydrogeology of the chalk of north-west Europe*. Oxford:
656 Clarendon Press. 35-58.

657 Price, M., R. G. Low, and C. McCann (2000), Mechanisms of water storage and flow in the
658 unsaturated zone of chalk aquifer, *J. Hydrol.*, 54-71.

659 Rawls, W. J., D. L. Brankensiek, and K. E. Saxton (1982), Estimation of soil water
660 properties, *Trans. ASAE*, 25(5), 1316–1320.

661 Robinson, E. L., E. Blyth, D. B. Clark, J. Finch, and A. C. Rudd (2015), Climate hydrology
662 and ecology research support system potential evapotranspiration dataset for Great Britain
663 (1961- 2012) [CHESS-PE], NERC-Environmental Information Data Centre.

664 Schär C., D. Lüthi, U. Beyerle, and E. Heise (1999), A soil precipitation feedback: A process
665 study with a regional climate model, *J. Clim.*, 12, 722–741.

666 Schaap, M. G., and F. J. Leij (1998), Database-related accuracy and uncertainty of
667 pedotransfer functions, *Soil Sci.*, 163(10), 765–779.

668 Sorensen, J. P. R., J. W. Finch, A. M. Ireson, and C. R. Jackson (2014), Comparison of varied
669 complexity models simulating recharge at the field scale, *Hydrol. Process.*, 28, 2091-2102.

670 Van den Daele, G. F. A., J. A. Barker, L. D. Connell, T. C. Atkinson, W. G. Darling, and J.
671 D. Cooper (2007), *J. Hydrol.*, 342, 157-172.

672 Van Genuchten, M. Th. (1980), A closed-form equation for predicting the hydraulic
673 conductivity of unsaturated soils, *Soil Sci. Soc. Am. J.*, 44, 892–898.

674 Walters, D. N., K. D. Williams, I. A. Boutle, A. C. Bushell, J. M. Edwards, P. R. Field, A. P.
675 Lock, C. J. Morcrette, R. A. Stratton, J. M. Wilkinson, M. R. Willett, N. Bellouin, A. Boda-
676 Salcedo, M. E. Brooks, D. Copsey, P. D. Earnshaw, S. C. Hardiman, C. M. Harris, R. C.
677 Levine, C. MacLachlan, J. C. Manners, G. M. Martin, S. F. Milton, M. D. Palmer, M. J.
678 Roberts, J. M. Rodríguez, W. J. Tennant, and P. L. Vidale (2014), The Met Office unified
679 model global atmosphere 4.0 and JULES global land 4.0 configurations, *Geosci. Model Dev.*,
680 7, 361-386.

681 Welliings, S. R., and J. P. Bell (1980), Movement of water and nitrate in the unsaturated zone
682 of upper chalk near Winchester, Hants., England, *J. Hydrol.*, 48, 119-136.

683 Williams, K., and D. Clark (2014), Disaggregation of daily data in JULES (Hadley Centre
684 technical note 96), Hadley Centre, Met Office, UK.

685 Zehe, E. and G. Blöschl (2004), Predictability of hydrologic response at the plot and
686 catchment scales: Role of initial conditions, *Water Resour. Res.*, 40.

687 Zehe, E., T. Maurer, J. Ihringer, and E. Plate (2001), Modeling water flow and mass transport
688 in a loess catchment, *Phys. Chem. Earth (B)*, 26, 487-507.

689 Zehe, E., U. Ehret, T. Blume, A. Kleidon, U. Scherer, and M. Westhoff (2013), A
690 thermodynamic approach to link self-organization, preferential flow and rainfall-runoff
691 behaviour, *Hydrol. Earth Syst. Sc.*, 17, 4297-4322.

692
693
694

695

696 **Tables**

697 Table 1. Field measurements and remote sensing data.

Data	Spatial scale	Temporal extent	Frequency	Source
Soil moisture	Point ^a	2003-2005	15 day	N. Hewitt (CEH)
Latent heat flux	Global	2006-2011	8 day, 1 month	MODIS
Discharge	Point ^b	2006-2011	1 day	NRFA

698 ^aMeasured at Warren Farm.699 ^bLocations are shown in Figure 1a.700 Table 2. Hydraulic properties for different soil types (refer to Figure 1c). Saturated hydraulic
701 conductivity (K_s) and porosity data are obtained from *Rawls et al.* [1982]. The Van Genuchten
702 parameters are acquired from *Schaap and Leij* [1998].

Texture	K_s (mm-d ⁻¹)	Porosity (-)	α (m ⁻¹)	n (-)
Loam	320	0.463	3.33	1.56
Silt loam	172	0.50	1.2	1.39
Clay	15	0.475	2.12	1.2

703

704 Table 3. Hydraulic properties of chalk

Properties	Uncalibrated		Range for calibration	Calibrated value
	Value	Source		
K_s (mm-d ⁻¹)	1.0	Price et al., 1993	0.2 - 25.0	0.31
S_0 (-)	0.8	Observations	0.0 - 1.0	0.46
f_m (-)	1×10 ⁵	Price et al., 1993	1×10 ⁴ - 1×10 ⁶	1×10 ⁵ *
α (m ⁻¹)	3.0	Le Vine et al., 2016	-	-
n (-)	1.4	Le Vine et al., 2016	-	-

705 * f_m parameter not calibrated706 Table 4. Comparison between observed and simulated daily average runoff from the two
707 configurations over the Kennet catchment. [Metrics include the Runoff Ratio \(RR\), relative bias \(\$\Delta\mu\$ \),](#)
708 [and relative difference in standard deviation \(\$\Delta\sigma\$ \) \(refer to appendix for further information\).](#)

Metric	Observed	Simulated (default)	Simulated (macro)
RR	0.40	0.82	0.460.37
$\Delta\mu$	-	1.04	0.12-0.05
$\Delta\sigma$	-	2.04	0.650.70

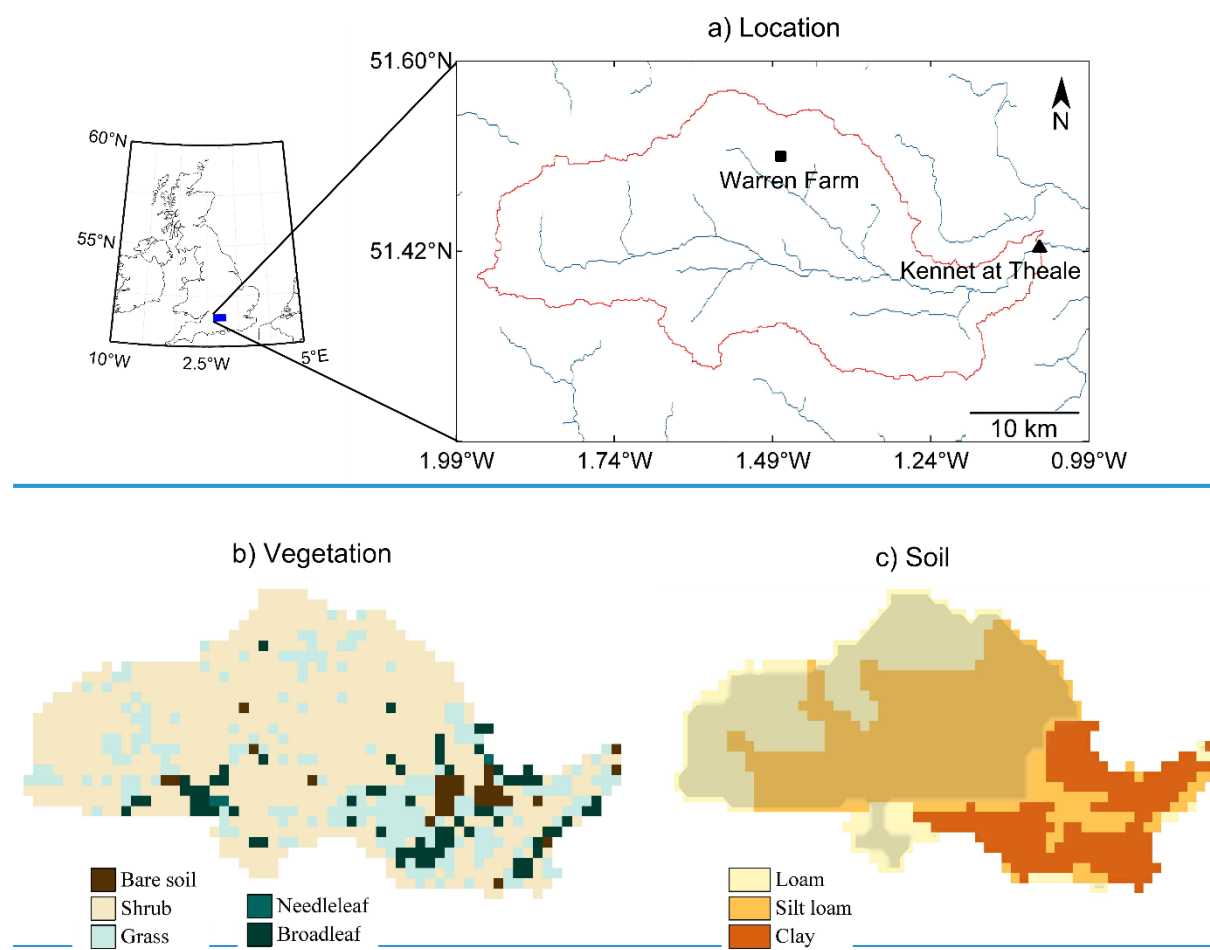
709

710

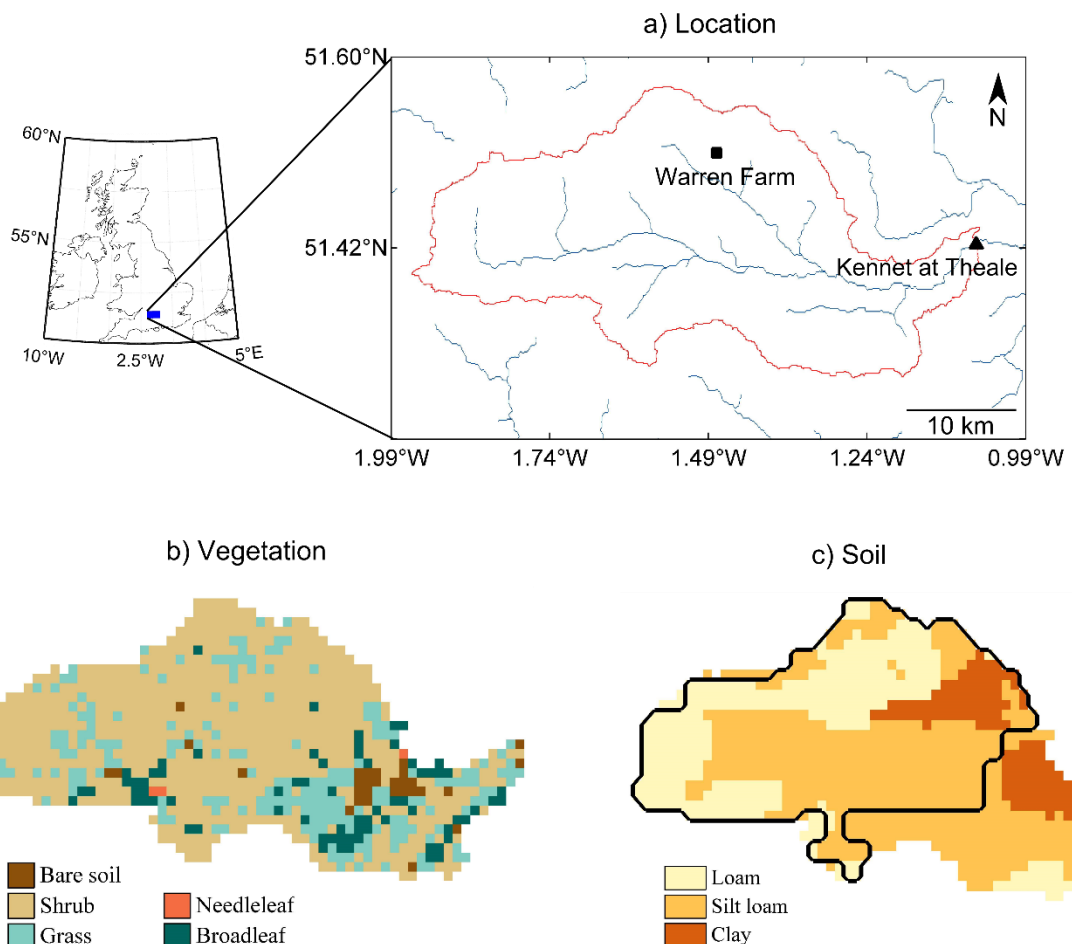
711

712 **Figures**713 Figure 1. [\(a\)](#) Location [\(a\)](#), [\(b\)](#) vegetation cover [\(b\)](#), and [\(c\)](#) soil texture [\(c\)](#) over the study area.

714 The red line in (a) outlines the Kennet catchment boundary, while the river network is shown
 715 in blue. The black triangle in (a) shows the location of the discharge gauging station at the
 716 catchment outlet [and while](#) the black square corresponds to Warren Farm location where
 717 point-scale simulations are carried out. [The black line in \(c\) encloses the area of the](#)
 718 [catchment where chalk is present. The shaded area in \(c\) represents the location of chalk in](#)
 719 [the catchment.](#)



720



721

722

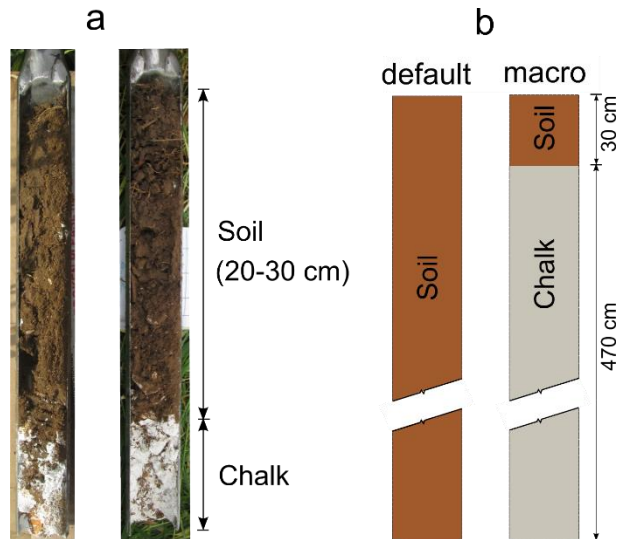
723

724

725 Figure 2. (a) Example of soil profiles collected at Warren Farm during a field campaign in
 726 2015 (a), and (b) the two model configurations (b).

727

728



729

730

731

732

733

734

735

736

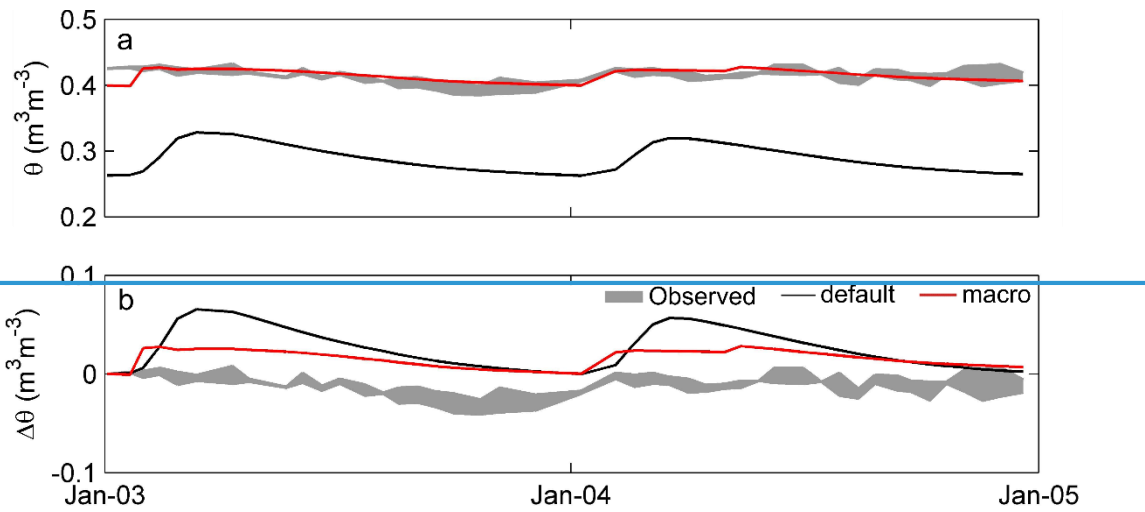
737

738

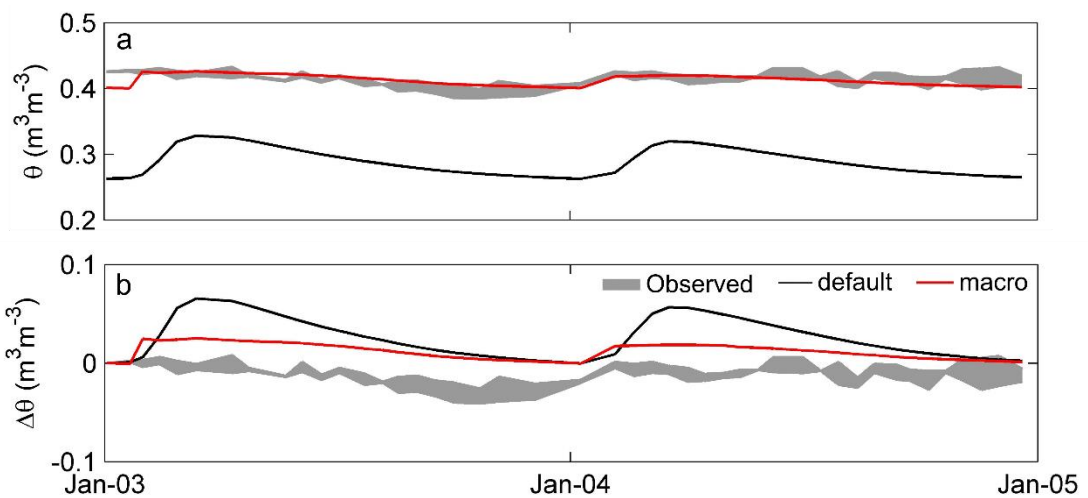
739

740 Figure 3. Comparison between observed and simulated (a) soil moisture (θ) and (b) change in
741 soil moisture ($\Delta\theta$) from the *default* and *macro* configurations at a depth of 2_m below land

742 surface [at the Warren Farm site](#). The shaded areas constructed from 2 soil moisture probes at
743 the Warren Farm site denote the range of observed data in these plots.



744
745



746
747

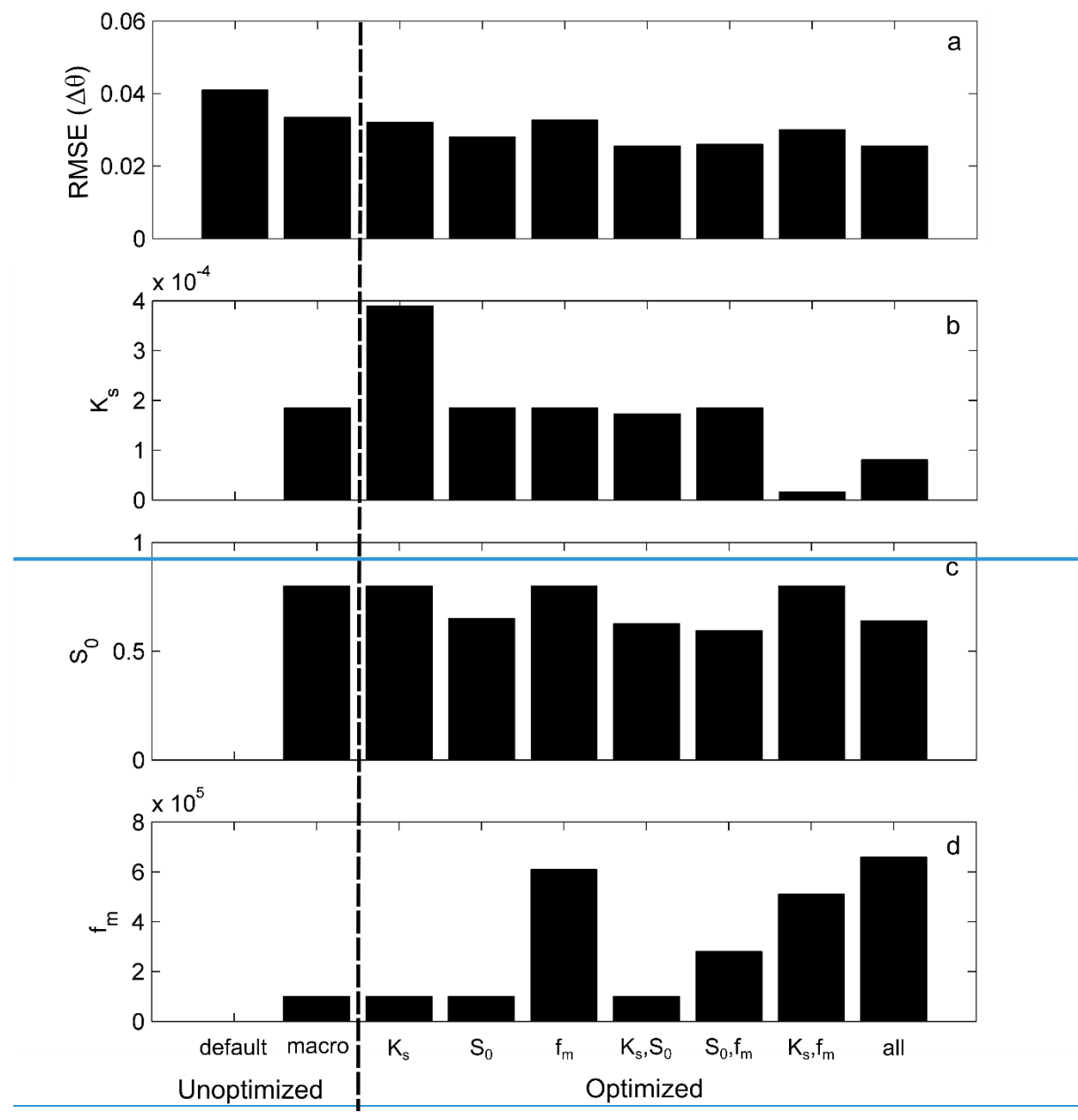
748
749

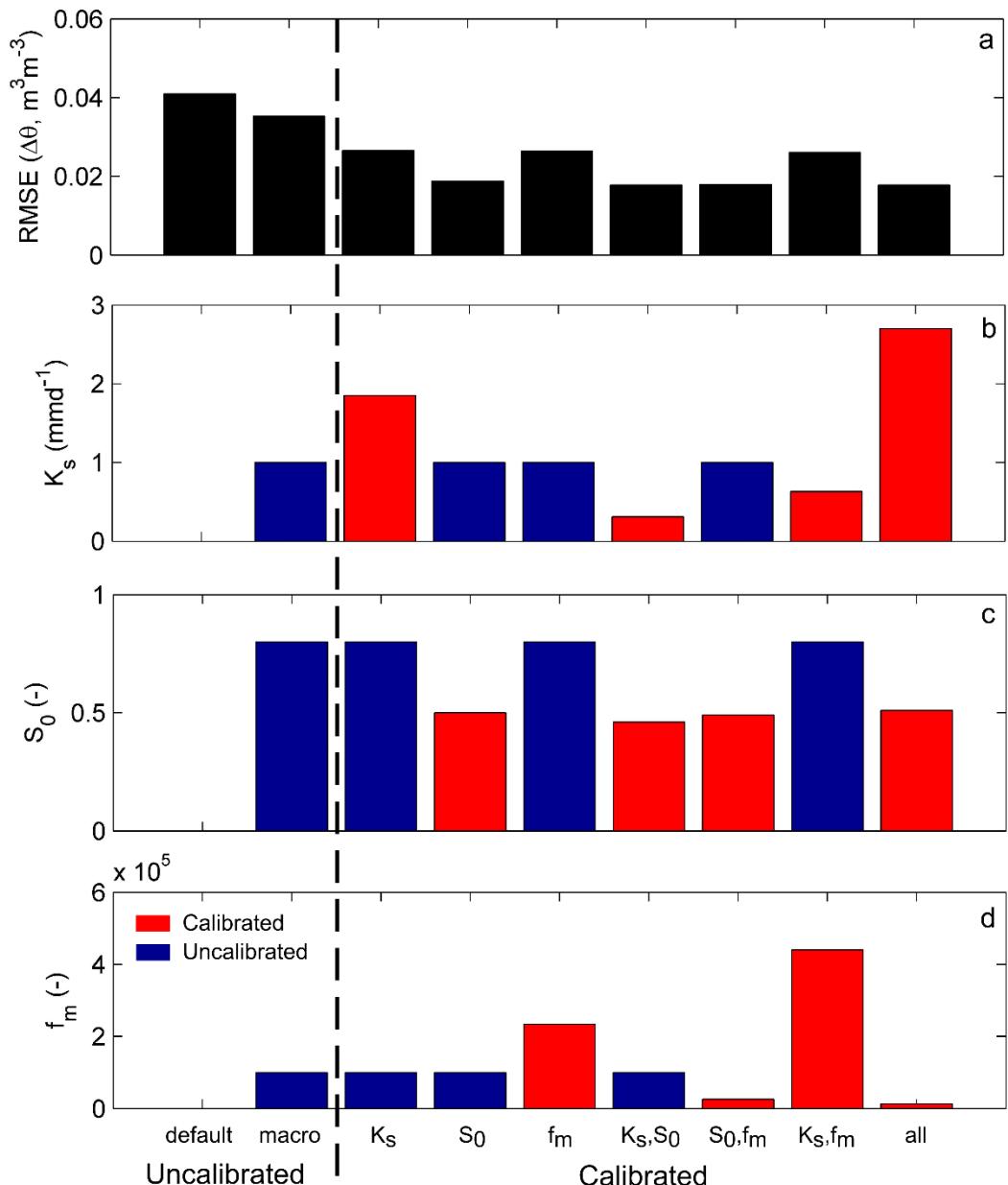
750

751
752
753
754
755

756 Figure 4. (a) Model performance in reproducing observed and simulated $\Delta\theta$, (b) K_s , (c) S_o and
757 (d) f_m for various different parameter combinations considered in the optimization. For each
758 parameter (i.e., panels b, c, and d), red bars show cases in which the relevant parameter is
759 calibrated (either individually or in combination with others); while the blue bars correspond
760 to cases in which the selected parameter is not calibrated (i.e., fixed value according to
761 literature as in the *macro* case)The uncalibrated model parameter values are shown in blue
762 while red shows the calibrated values in b, c and d. Note that except for the *default* and
763 *macro*, the simulation yielding the lowest RMSE (out of 2,000 model runs) is presented in
764 this plot.

765

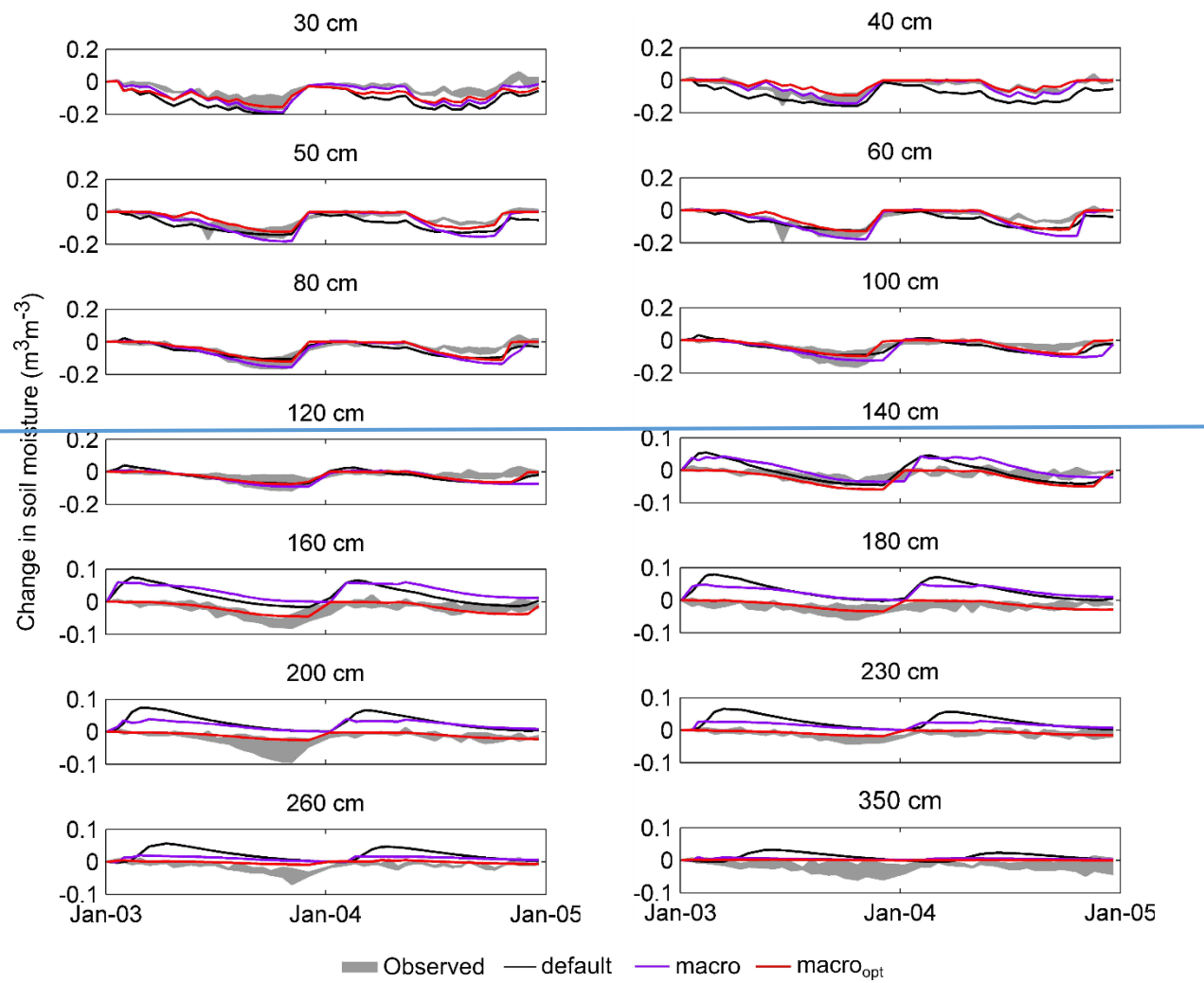


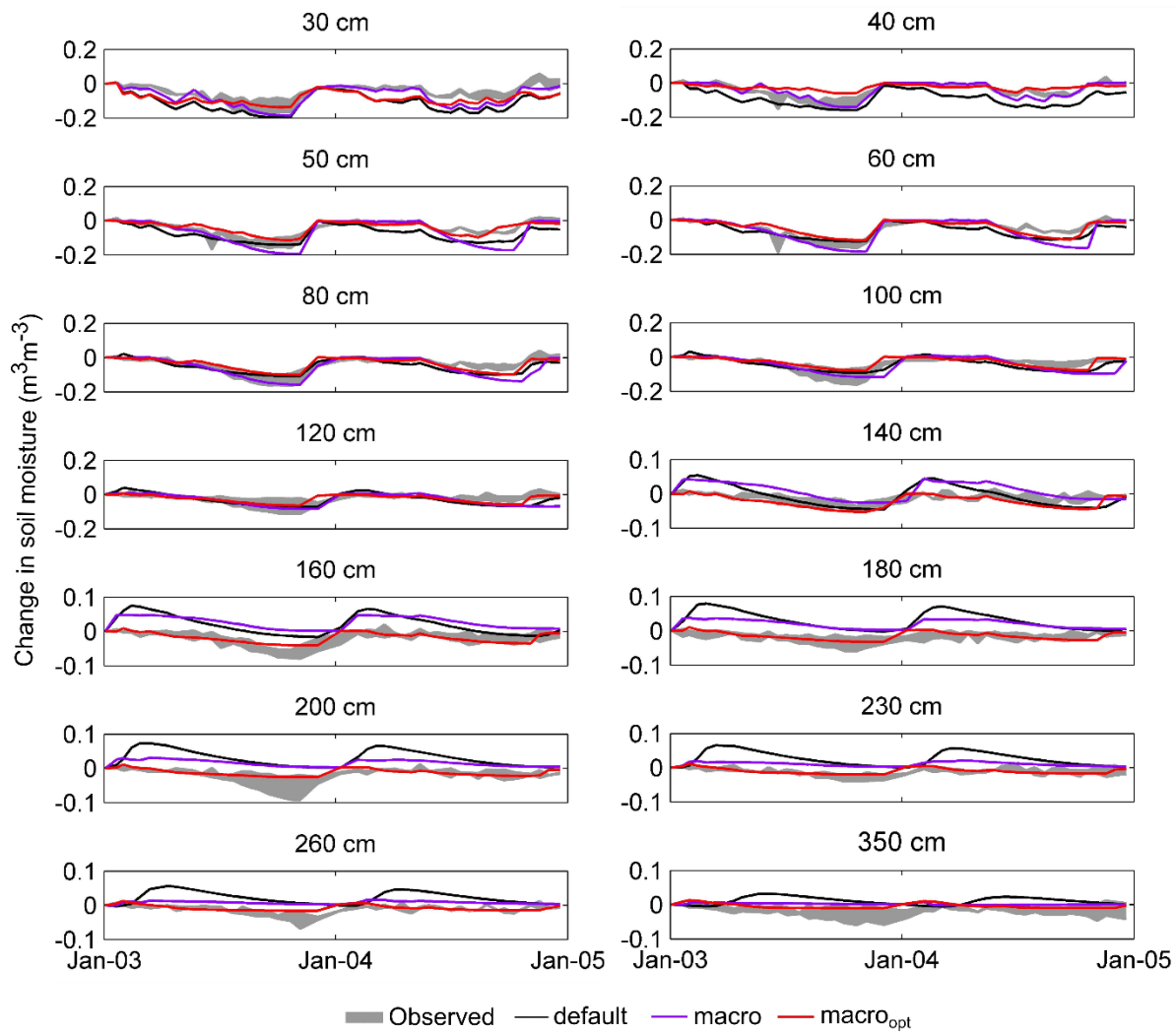


767

768 Figure 5. Comparison between observed and simulated $\Delta\theta$ from *default*, *macro* and $macro_{opt}$
 769 configurations at various depths below land surface. The shaded areas, which are is
 770 constructed from 2 soil moisture probes at the Warren Farm site, denotes the range of $\Delta\theta$.

771





773

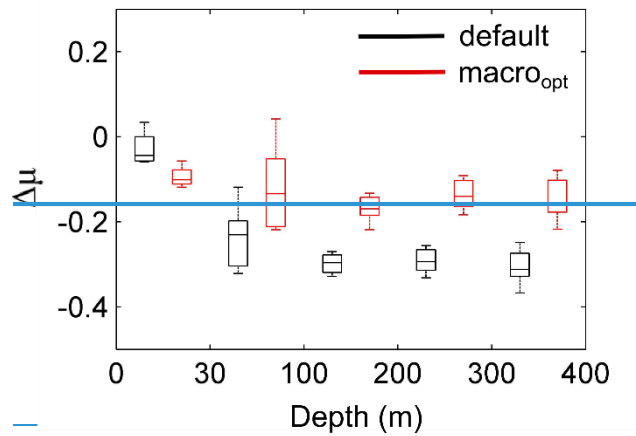
774

775

776

777 [Figure 6. Box plot of relative bias \(\$\Delta\mu\$ \) of simulated soil moisture from *default* and *macro*](#)
 778 [configurations at different depth ranges shown in individual intervals \(e.g., 0-30 cm, 30-100](#)
 779 [cm, and so on\).](#)

780



781
782

783

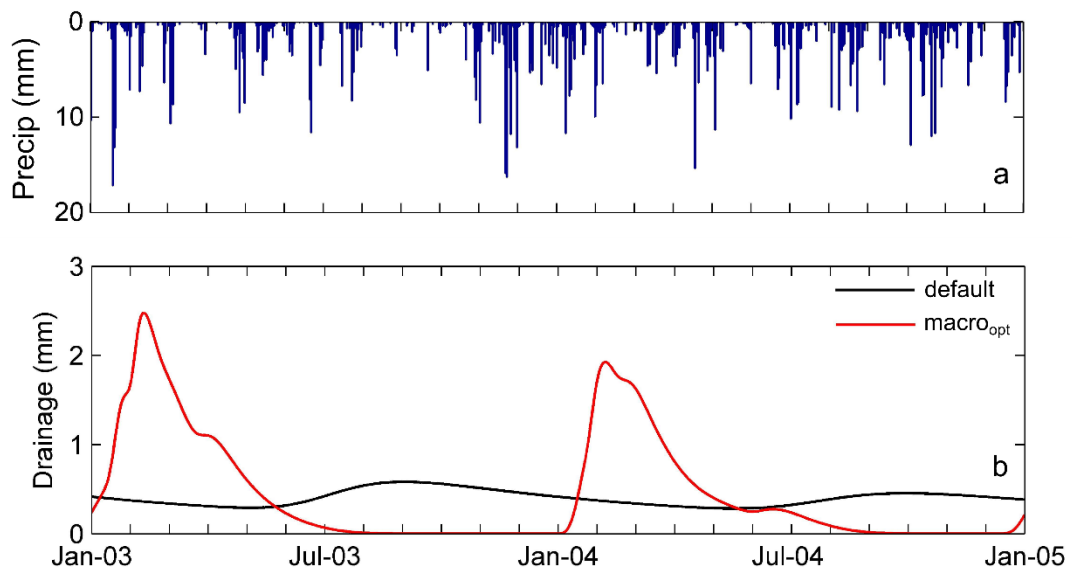
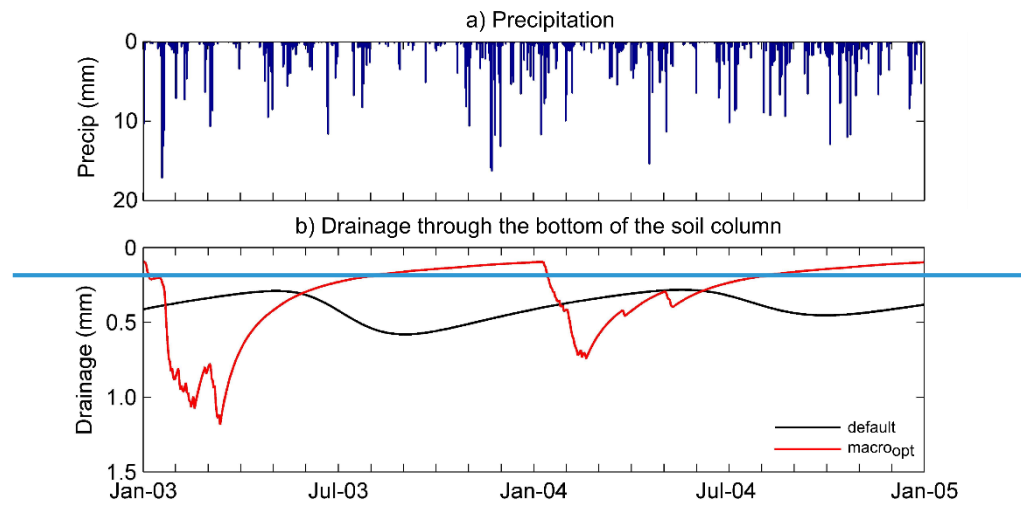
784
785

786

787
788
789
790
791
792

793 Figure 76. (a) Daily precipitation and (b) daily sum-of-drainage through the bottom of the
794 soil column at Warren Farm over the two simulated years (2003-2005).

795



797

798

799

800

801

802

803

804

805

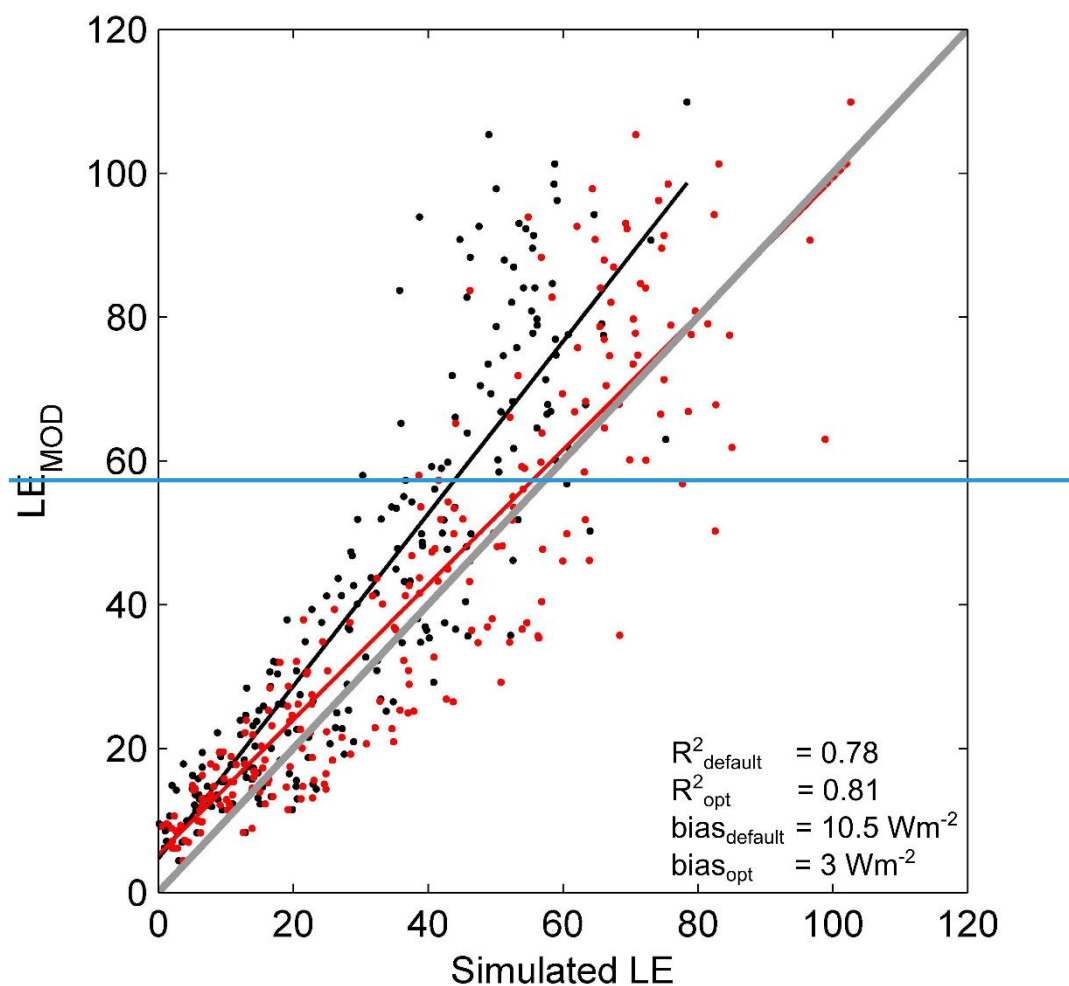
806

807

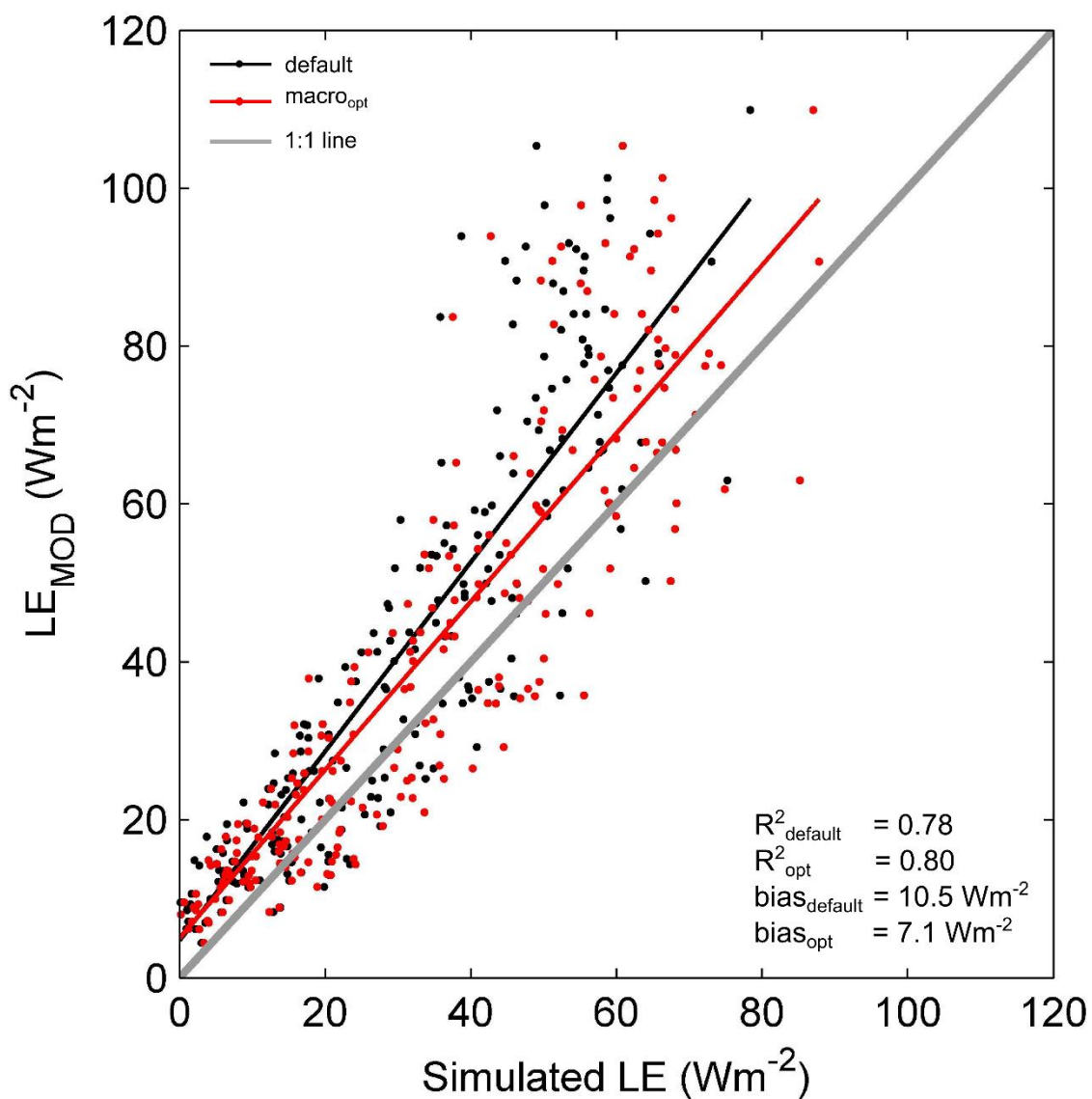
808

809 Figure 87. Catchment average 8 day composites of MODIS estimated LE (LE_{MOD}) against
810 simulated LE from *default* and *macro* configurations ($LE_{default}$ and LE_{macro} , respectively) along
811 with the linear models fitted for $LE_{default}$ (black line) and LE_{macro} (red line). The 1:1 line is
812 shown in grey, which represents the perfect fit between LE_{MOD} and simulated LE .

813



814

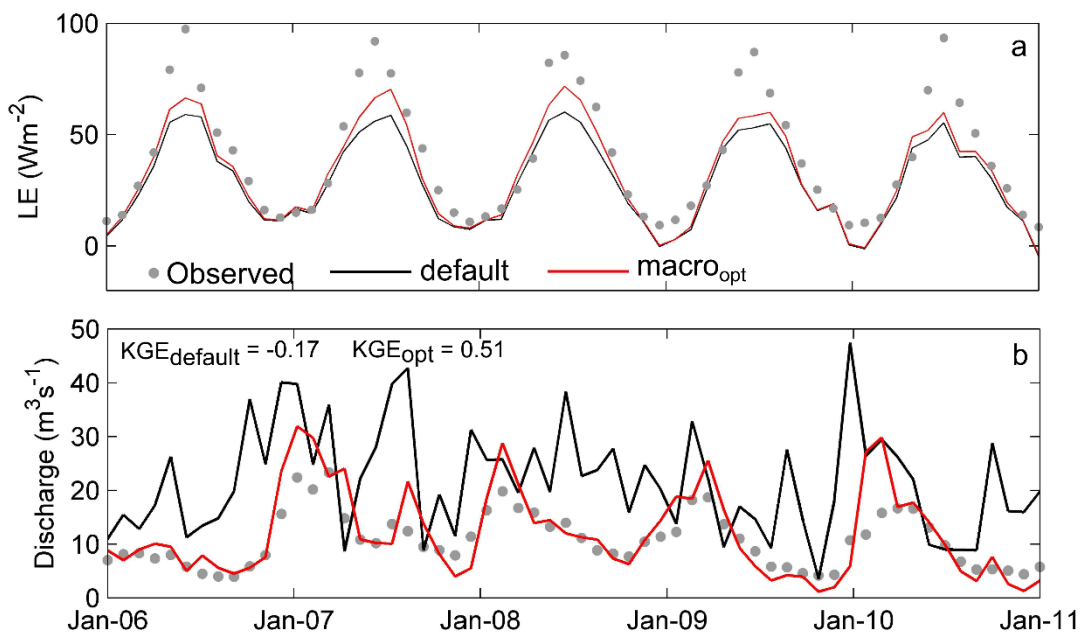
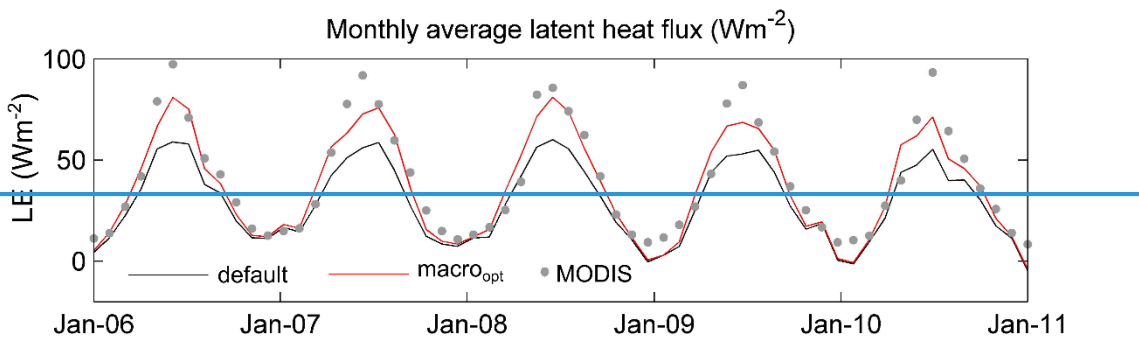


815
816

817

818 Figure 98.(a) Spatially averaged monthly latent heat flux (LE) from MODIS, *default* and
819 *macro_{opt}* configurations over the Kennet catchment [and \(b\) monthly average observed and](#)
820 [simulated discharge from the *default* and *macro_{opt}* configurations at the ‘Kennet at Theale’](#)
821 [gauging station.](#)

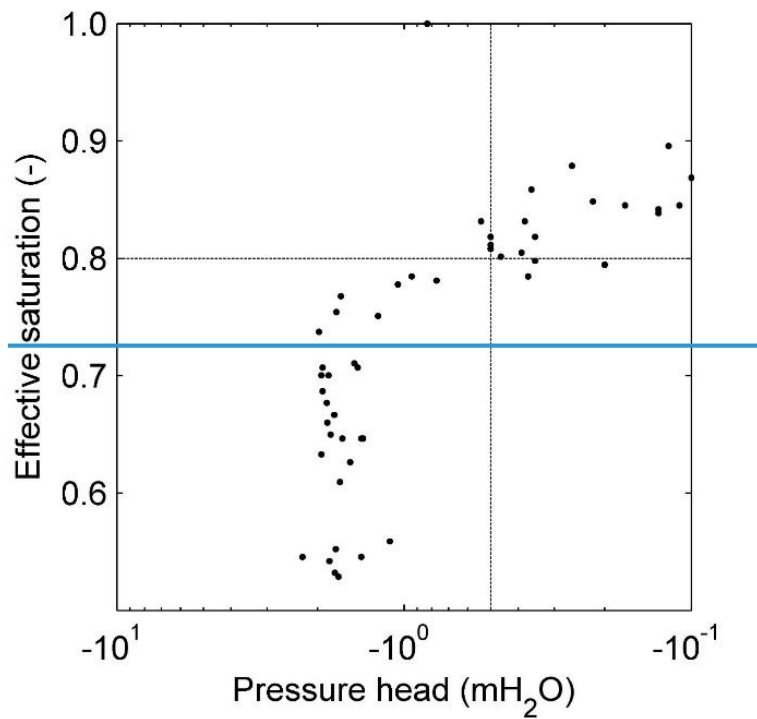
822



831
832
833
834
835
836
837
838
839

Supplementary materials

Figure S1. Saturation-pressure head relationship (May 2003–December 2005) at Warren Farm measured fortnightly at 40 cm below land surface. (Source: Ned Hewett, CEH, personal communication).



840
841
842

843
844
845
846
847
848
849
850
851
852
853

